Thermal Science and Engineering Progress 56 (2024) 103025

Contents lists available at ScienceDirect

Thermal Science and Engineering Progress

journal homepage: www.sciencedirect.com/journal/thermal-science-and-engineering-progress

Exploring heat exchange in space: Recent advances in two-phase fluid experiments in microgravity

Glauco Nobrega [a,b], Inês Santos Afonso [a,b], Beatriz Cardoso [a], Reinaldo Rodrigues de Souza [a,c], Ana Moita [c,d], João Eduardo Ribeiro [b,e], Rui A. Lima [b,f,g,*]

[a] Mechanical Engineering and Resource Sustainability Center (MEtRICs), Mechanical Engineering Department, University of Minho, Campus de Azurém, 4800-058 Guimarães, Portugal

[b] Centro de Investigação de Montanha (CIMO), Instituto Politécnico de Bragança, Campus de Santa Apolónia, 5300-253 Bragança, Portugal

[c] IN+, Center for Innovation, Technology and Policy Research, Instituto Superior Técnico, Universidade de Lisboa. Av. Rovisco Pais, 1049-001 Lisboa, Portugal

[d] CINAMIL - Centro de Investigação Desenvolvimento e Inovação da Academia Militar, Academia Militar, Instituto Universitário Militar, Rua Gomes Freire, 1169-203 Lisboa, Portugal

[e] Instituto Politécnico de Bragança, Campus de Santa Apolónia, 5300-253 Bragança, Portugal

[f] CEFT, Transport Phenomena Research Center, Faculty of Engineering, University of Porto (FEUP), R. Dr. Roberto Frias, 4200-465 Porto, Portugal

[g] ALiCE - Associate Laboratory in Chemical Engineering, Faculty of Engineering, University of Porto, Rua Dr. Roberto Frias, 4200-465 Porto, Portugal

A R T I C L E I N F O

Keywords:
Thermal control
Microgravity
Flow boiling
Vapor compression cycle
Pool boiling
Heat pipe
Phase change material

A B S T R A C T

Thermal regulation has assumed a central role in space expeditions ever since the inception of Sputnik-1 in 1957. Throughout the years, numerous techniques have been developed to regulate temperatures in spacecraft and space habitats. Initially, passive systems like heat shields and thermal linings were employed, while newer missions embrace active cooling using fluids like ammonia and water. With significant advancements in lunar exploration, thermal management systems have been integrated to ensure effective heat protection and dissipation. Experiments carried out in drop towers, parabolic flights, sounding rockets, and aboard the International Space Station (ISS) have yielded valuable insights into the physics of fluids, pool boiling, boiling in two-phase flow, and cooling phenomena. However, conducting tests in microgravity conditions can lead to lower performances, and accurate numerical simulations remain a challenge. At present, various organizations are conducting research to drive progress in thermal management and enhance the technology of space devices. This review describes the most recent advances in two-phase fluid experiments in microgravity. Furthermore, the major challenges that persist in this field are presented and discussed, along with observations on trends and possibilities for the future of thermal control in space. This review attempts to be a relevant guide for future research and developments on thermal control in space.

1. Introduction

Thermal control was established as a pivotal element of space expeditions ever since the beginning of the inaugural man-made satellite (Sputnik-1) being placed into low-Earth orbit, accomplished by the Soviet Union in 1957. This satellite, designed by Sergej Pavlovich, featured a heat shield constructed from AMG6T alloy and to regulate the temperature, the satellite was filled with dry nitrogen at a pressure of 1.3 atm. Additionally, a dual thermal switch was implemented, whereby a fan would activate if the temperature exceeded 36 °C and deactivate once the temperature dropped below 20 °C [1]. Sputnik 2, in turn, featured two thermal control systems for the instruments, as well as one for the dog Laika. However, a problem with the separation of spacecraft components during orbital entry prevented the proper functioning of the thermal control system, resulting in temperatures reaching 40 °C and ultimately leading to the demise of the animal after approximately two days [2].

Explorer 1, the inaugural satellite dispatched by the United States, was furnished with three external resistance thermometers and one internal thermometer. Its main objective was to evaluate the efficiency of passive temperature control through insulating materials and an exterior coating. [3] and remained in operation for a period of three months [4]. In 1960, *Heller* [4] expressed concerns about the thermal control of exploratory satellites and identified parameters that should be taken into consideration, such as orbital characteristics, material properties of

* Corresponding author at: Metrics, Mechanical Eng. Depart.t, University of Minho, Campus de Azurém, 4800-058 Guimarães, Portugal.
E-mail address: rl@dem.uminho.pt (R.A. Lima).

https://doi.org/10.1016/j.tsep.2024.103025
Received 21 July 2024; Received in revised form 24 September 2024; Accepted 30 October 2024
Available online 1 November 2024

Nomenclature

Bo	Boiling number
D_{eq}	Equivalent heated diameter
Fr_θ	Orientation-specific Froude number
G	Mass Velocity
g	Gravitational acceleration
L_h	Length
Oh	Ohnesorge number
Nu	Nusselt number
q''_{CHF}	Critical Heat Flux
x	Vapor quality
x_e	Thermodynamic equilibrium quality
We	Weber number

Greek symbols

α	Heat transfer coefficient
θ	Orientation angle of channel
ρ	Density
σ	Surface Tension

Subscripts

CHF	Critical Heat Flux
D_e	Channel diameter
f	saturated liquid
g	saturated vapor
in	Channel heated section inlet; inlet
LO	Liquid Only
TP	Two phase Fluid

Acronyms

CCD	Camera charge-coupled device
CFD	Computational Fluid Dynamics
CHF	Critical heat flux
CASCo	*Code Avancé de Simulation du Caloduc Oscillant*: Advanced PHP Simulation Code
DEP	Dielectrophoretic
DLR	German Aerospace Center
EHD	Electrohydrodynamic
ESA	European Space Agency
FBCE	Flow Boiling and Condensation Experiment
FBM	Flow Boiling Module
FEM	Finite Element Method
FPPHP	Flat Pulsating Heat Pipe
FPS	Frames per second
ISS	International Space Station
JAXA	Japan Aerospace Exploration Agency
LEO	Low Earth Orbit
MPTL	*M*echanically *P*umped *T*wo-phase *L*oop
PCM	Phase Change Material
PDMS	Polydimethylsiloxane
PTFE	Polytetrafluoroethylene
TRL	Technology Readiness Level
UDF	User-defined function
VCC	Vapor Compression Cycle
VOF	Volume of Fluid
ZARM	German Center for Applied Space Technology and Microgravity

the spacecraft, sun direction, and albedo radiation, among others. It was concluded that satellites could have their temperature regulated through passive systems.

The first cosmonaut in history, Yuri Gagarin, aboard the Vostok 1 spacecraft, had two fans in his suit: one for air circulation in his helmet and another for body cooling [5]. Within the cabin, Gagarin could set a reference temperature since a heat exchanger was connected to a radiator in the instrument module through a liquid circuit [6]. The International Space Station (ISS) features two active cooling systems: one utilizing ammonia and the other employing water. These systems enable the removal of heat from both the equipment and the internal spaces where the crew circulates [7].

More recently, advances in research have highlighted lunar exploration. For instance, in the case of the Chang'E-5 lunar module, which comprises a lunar landing module and a lunar ascension vehicle, a comprehensive and self-governing thermal management system was devised. This system encompassed a single-phase water circuit and a high-temperature heat protection shield.[8]. Nevertheless, there are several pivotal aspects pertaining to this subject that have not been documented in typical research papers, as already emphasized in the introduction of Karan's publication [8] with a cautionary note in 1998. and the total information about the technology applied continuous being keep as unduplicated material due the economic and military advantage that have this type of information provide. The access to aerospace technology is also undesired by the countries who already have some control of the technology due the space traffic management, and cybersecurity. On the other hand, the huge decrease of the price from $18,500 (between 1970–2000) to $2,720 per kilogram must increase the number of objects in the space turning this technology more available [9].

Thermal control in space covers different equipment and situations, as summarized in Fig. 1, and requires special attention that is different from what is usually used in terrestrial systems. It is necessary to have not only temperature control, but also uniformity and stabilization of the same. Among the main restrictions for thermal control, the vacuum, the thermal environment, gravity, and space radiation stands out, making radiation the only possible way to remove heat in the vast majority of space missions. These factors experience significant fluctuations depending on the proximity of celestial bodies, their respective orbits, altitudes, configurations, geometries, and the characteristics of

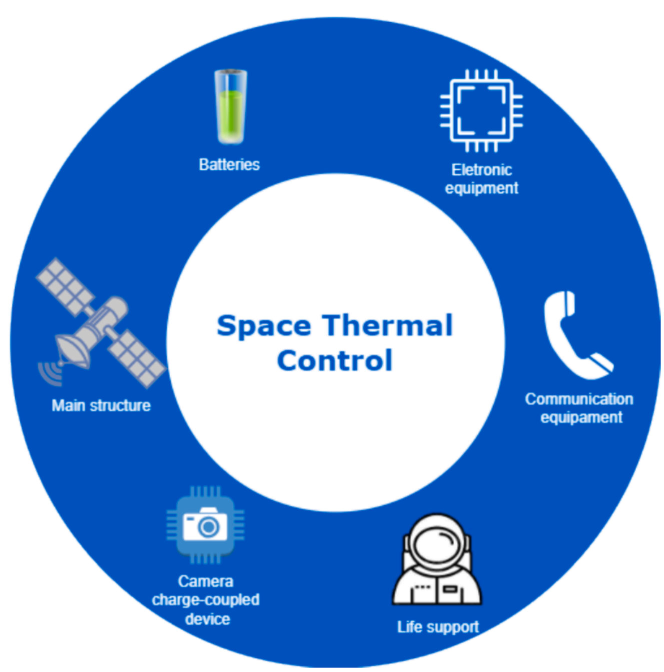

Fig. 1. Equipment that needs thermal control in space.

radiation emission and reception, among other considerations. Beside this, different atmospheres are still poorly known, leading to the need for an oversized thermal control configuration [10].

In a satellite, the entire exterior, including colours, shape, and orientation, is designed in a way that allows operation within the desired temperatures, which should be as close as possible to the temperatures used during its construction, ideally resembling comfortable temperatures on Earth [8]. Furthermore, it is necessary for the spacecraft to have high emissivity on the side facing the Sun and low emissivity in the direction radiating into space [11]. Small satellites, especially, face even greater challenges in terms of cooling. Their small mass makes them more reactive to environmental changes, and the surface area available for radiators, solar panels, and instrument doors is significantly limited. The volume limitation also affects the space available for heat exchangers, which, in turn, restricts the power that could be allocated to enhancing heat exchange [12,13]. Cooling becomes particularly problematic for CubeSats due to their small size, mass, and high thermal density, coupled with a very limited available area for heat exchange. In some of the most critical cases, only 25 % of the available area is allocated for heat exchange [14].

In addition to issues of difficulty regarding the environment, total power usage as well as density has tended to increase in spacecraft and there are restrictions on both maximum and minimum temperatures, for example, the temperature range of electronic equipment must stay between −15 to 50 °C[10]. In addition to equipment considerations, when a human is present inside the spacecraft, there are additional criteria to be considered for temperature control. Not only must the local atmospheric temperature be regulated, but also the temperature of food and even bodily fluids for potential future testing[15]. In the orbital region of the ISS (370–460 km), temperatures at surfaces exposed to the sunlight can range from 500 to 2000 °C [16].

The production of heat in space is of great complexity: in spacecraft, it can reach hectowatts or kilowatts, while for nanosatellites, depending on its specific design, mission requirements, and the systems onboard, the power consumption of a typical nanosatellite ranges between 5 and 20 W. The heat flux in high-power microwave equipment and laser pumping sources can reach hundreds of Watts per square meter [10].

Several aspects have been recently studied, with particular focus on microgravity. Hu & Kang, [17] compiled experiments conducted aboard the Chinese experimental satellite SJ-10, which orbited in Low Earth Orbit (LEO) for 12 days. The focus of these experiments was to study fluid physics in microgravity and address biological questions. Brendel et al. discussed vapor compression refrigeration in microgravity environments highlighting the gaps in the literature as the lack of details regarding tested devices[7]. Ali conducted a review on heat pipes with Phase Change Materials (PCM) and demonstrated that the overheating issue in heat pipes and the low thermal conductivity of PCMs can be overcome through their combination [18]. *Yost & Weston* [12] presented a comprehensive state-of-the-art review on small satellites, addressing key points regarding this emerging trend, including thermal control. *Sielaff* [19] provided an overview of the research conducted in the Multiscale Boiling Project (also referred to as RUBI) between 2019 and 2021 on the ISS, focusing on the effects of shear flow, electric fields, and their combination. In 2021, *Wang* et al. [20] discussed aerospace-oriented spray cooling technology, recognized as one of the next-generation cooling technologies, with a potential performance of up to 825 W/m^2. *Liu* et al. [21] reviewed spray cooling techniques applied to heat transfer in the aerospace field. *Weislogel* et al. [22] described some of the challenges encountered in fluid transport on the space station due to the absence of buoyancy forces, and capillary solutions were presented. *Konishi & Mudawar* [23] conducted a review on flow boiling in space. A review on flow boiling and pool boiling in microgravity environments was carried out by *Hong* et al. [24], with a particular emphasis on the models used to forecast the outcomes.

Recently, significant efforts have been made to better understand phase change cooling phenomena with the dual goals of expanding knowledge of the phenomenon without buoyancy forces and to explore ways of enhancing its efficiency and develop heat exchangers with improved predictability of their effectiveness. In this regard, various tests are being conducted at the Flow Boiling Module (FBM) on the ISS [25].

The Japan Aerospace Exploration Agency (JAXA) collaborates with universities and institutes in conducting numerous studies [26]. Additionally, drop tower experiments and parabolic flight campaigns, especially in China, the European Union, and the United States, are being carried out to gain a deeper understanding of the underlying physics and facilitate the development of more efficient and suitable technologies for specific applications. According to *Sridhar* [27], even in terrestrial conditions, the next generation of heat exchangers will move away from the conventional techniques such as natural or forced convection and instead focus on more efficient tools like phase-change cooling. Within this context, this review provides the most recent cooling methods involving the phase-change of refrigerants. Therefore, this review aims to gather experiments with two-phase fluids conducted in microgravity environments or microgravity analogues. To the best of our knowledge, this will be the first time a work summarizes and addresses the main experiments conducted in this environment for two-phase fluids, focusing on the experimental setup, as well as the main results and conclusions obtained for technologies such as Pool Boiling, Flow Boiling, Heat Pipes, Vapor Compression Cycle, and Phase Change Material in English and available at Web of science published since the Falcon Heavy rocket launched a car into space in 2018, marking a new era in space missions where private companies are sharing the spotlight with government space agencies. The present review article seeks to map recent discoveries, identify major challenges that persist in this field, observe recent trends and evaluate the potential of different forms of heat transfer in space. Understanding these technologies, their limitations, possibilities, and challenges is crucial to enabling the advancement of space exploration in adverse conditions, as well as to developing more efficient, safe, and reliable equipment, vehicles, and space suits.

A new perspective for this field is addressed beyond, with a great potential for an application that did not receive attention in previous years: nanofluids, which, with new techniques, have been demonstrating greater stability [28], thus enabling the design of fluids with improved thermal properties in heat exchangers used in space. The application of nanoparticles in PCMs is also evaluated. Furthermore, the possibility of using Polydimethylsiloxane (PDMS) for heat exchanger fabrication is demonstrated, considering its manufacturing flexibility, property alterations, and the potential to observe fluid behaviour.

2. Review of recent experiments performed in microgravity

Microgravity testing experiments can be conducted in drop towers, parabolic flights, sounding rockets, and objects in orbit [27,29]. Drop towers essentially enable experiments to be carried out in free fall, in a vacuum. More recent studies employ catapults to initiate the experiment from the ground level and extend the brief moments of microgravity encountered throughout the descent. Parabolic flights allow for the simulation of microgravity and the gravity of other celestial bodies with higher or lower gravity than Earth. Microgravity can be achieved for periods of 15 to 30 s. Sounding rockets reach an altitude of at least 100 km and provide a microgravity environment during their descent. Traditional rockets typically allow for tests lasting more than 10 min, while commercial rockets are limited to 3 min. Tests on objects in orbit with the International Space Station and satellites have the advantage of offering a microgravity environment for months [29].

More recently, Tsinghua University in Beijing developed a drop tunnel for microgravity testing, providing a period of 2.2 s of microgravity within the Lee Shau Kee Science and Technology Building at a height of 35 m [30]. Table 1 identifies the forms of microgravity testing as well as other important characteristics. For testing gravity on other celestial bodies, there is, for example, a project called LUNA, funded by

Table 1
Examples of testing platforms based on [29] with updated data from [30].

Platform	μg time	Space/Volume for payload	Mass for payload (kg)	Cost in US $	Possibility for manual intervention
Inclined stand	Not Applicable	1.7 m^3	100	10,000	High – experiment can be manually accessed at any time
Drop tunnel	2.2 s	Not available	280 (capsule included)	Not available	Low – usually impossible
Drop tower	9.3 s	0.34 m^3	162		Low – usually impossible
Parabolic Flight	20–30 s	Area of 3x3m	Not available	~38500	High – researchers can intervene in experiment
Commercial sounding rocket	3 min	0,052 m^3	11.3	~115000	Low – usually impossible
Orbital spacecraft	Several months	~0.2 m^3	~165	Not available	Low – usually long-term experiments should be operated remotely to save crew time

the German Aerospace Center (DLR) and the European Space Agency (ESA), which involves constructing a lunar mock-up near Cologne, Germany. In this mock-up, scientists conduct experiments simulating lunar gravity using crane systems and pulleys [31].

Due to limitations in cost, time and operational conditions, there are assessments that can potentially validate the independence of gravity in the system, such as tests at various inclinations [29]. In 2020, *Liu* et al. [32] created a technique to use ground-based experiments to evaluate subcooled flow boiling in microgravity. The authors suggest conducting experiments at inclinations of 135 and 315 degrees, which provide good accuracy in determining the critical heat flux (CHF). Based on Newton's first law, the authors aimed to nullify buoyancy forces by tilting the cooling plane.

Other difficulties are encountered in these tests. For instance, *Inoue* et al. [33] warn that it is not possible to use the same equipment and environmental conditions for tests on Earth and in space. Additionally, the avionic airflow within the ISS leads to significant heat loss to the station's environment, raising an important question for tests conducted in that environment.

Yu et al. [34], in 2022, attempted to gather data on pressure and temperature in a wickless heat pipe. Despite employing the most advanced measurement techniques available, they were unable to observe the pressure and temperature satisfactorily during bubble formation. Furthermore, the high-speed camera used by *Mudawar* et al. [25] necessitates some form of cooling, typically with water.

This review addresses two active cooling technologies, flow boiling and Vapor Compression Cycle (VCC), as well as three passive cooling methods: PCM, pool boiling and heat pipes in particular. To facilitate the identification experiment characteristics as set-up and key results, the technology employed, the fluid used, and the test locations, data has been summarized in Table 2.

2.1. Pool boiling experiments in microgravity

Pool boiling is known to be a powerful cooling strategy, based on the change of a liquid into a vapor. In addition to latent heat, pool boiling also takes advantage of natural convection, induced convection and quenching occurring during nucleate boiling. Its applications are diverse, ranging from reactors to rockets. However, due to the interaction of all these phenomena, pool boiling heat transfer is rather complicated, and extensive research has been done not only to enhance its comprehension but also to attain improved control and efficiency [74]. The studies presented herein showcase various approaches aimed at enhancing nucleation phenomena, particularly through the utilization of electric fields, as well as gaining a better understanding of the disparities in these phenomena under terrestrial gravity and microgravity conditions.

Garivalis et al. [35] tested highly wettable microstructured surfaces and flat surfaces combined in parabolic flight. In comparison to the results for the flat surface on Earth's gravity, the results obtained for heat transfer showed a 53 % improvement. In their work, surfaces with micropillars were created on a silicon substrate to enhance near-wall capillary forces and an electric field with a potential difference of 15 kV was also applied, to move small bubbles away from the hot surface (Fig. 2).

Garivalis & Di Marco [44] tested the expansion of isolated bubbles when there is an electric field with a potential difference of up to 15 kV as shown in Fig. 3. It was observed that the electric field is capable of inducing bubble detachment, with a noteworthy impact that can be applied to enhance heat exchanger performance in space-oriented applications. In the experiment conducted aboard the ISS, it was found that as the intensity of the electric field increases, the contact angle and the size of the contact line also increase. The bubbles are directed toward the electrode and to regions where the electric field is weaker. In another study, *Bucci* et al. [45] presented experimental data for the bubble growth and detachment under a 15 kV electric field, which were evaluated using a high-speed camera aboard the ISS. It was observed that the increased electric field can explain an early release of bubbles trapped on the surface.

Castaneda et al. [40] evaluated the use of electrohydrodynamic (EHD) and dielectrophoretic (DEP) forces to maintain film stability during bubble nucleation, as buoyancy forces present in terrestrial gravity are absent in microgravity environments. The authors conducted tests during parabolic flights, and the results demonstrated that the use of electricity can increase the critical heat flux (CHF), decrease surface temperatures, and maintain boiling with low power consumption.

Romero-Calvo et al. [39] tested the use of magnetic polarization to induce phase separation in two-phase flow systems under microgravity conditions. The experiments were performed using air bubbles in different liquids, including water, manganese sulphate solution, culture broth, and olive oil. The results showed that the magnetic properties of the liquids were sufficient to allow for the collection and coalescence of air bubbles at specific locations, demonstrating the feasibility of dia- and paramagnetic phase separation methods in microgravity environments.

Saccone et al. [36] examined how gas bubbles inserted into FC-72 under various gravitational fields (0 g, ±1 g) were affected by an electric field produced by a potential difference of 25 kV. By pressing the bubble up against the surface, the dielectrophoretic force changed the bubble's shape. However, bubble removal was facilitated with the expansion of internal pressure. The vertical electric force operating on the bubble was experimentally determined, and a method was established to calculate the electric force on the bubble. The aim of the investigation was to determine whether an external electric field could be used to create a dependable and effective bubble removal system in space, where gravity is not present. Experiments were conducted under adiabatic and quasi-static conditions in different gravities, including microgravity obtained through parabolic flights. The study focused on the dynamics of momentum equilibrium terms, neglecting heat and mass transfer. They concluded that the electric force plays an important role in modifying the shape of the bubble and facilitating its removal under different gravitational fields.

Xue et al. [47] carried out research on coalescence, during pool

Table 2
Studies covered in this review.

Method	Fluid	Environment tested	Set-up	Key results	Reference
Pool boiling	FC-72	Parabolic flight	Surfaces with 10 μm high square micropillars	In microgravity, the combination of microstructured surfaces and electric field increases the critical heat flux (CHF) to 257 kW/m^2, exceeding the value in terrestrial gravity on flat surfaces.	[35]
Pool boiling	FC-72	Parabolic flight	0.5 mm circular hole in a stainless-steel plate with a 25 kV electrode 6 mm from the plate	Change in bubble shape due to dielectrophoretic force, facilitating removal.	[36]
Pool boiling	CO2	Drop tower	Dense cloud of bubbles generated in a cylindrical chamber with a diameter of 24.4 mm and a height of 200 mm	Identification of the three distinct stages of bubble growth in CO2-saturated water under microgravity conditions.	[37]
Pool boiling	FC-72	Drop tower	A millimeter-scale pyramidal cavity that employs capillary forces to retain the liquid–vapor meniscus	Independent of gravity levels, with three distinct operational modes of bubble growth identified	[38]
Pool boiling	Water, manganese sulfate solution, culture broth and olive oil	Drop tower	Becton-Dickinson BD Luer-Lok 30 ml syringes	The magnetic field was found to not only aid in bubble separation but also affect the interaction between bubbles and the container surfaces	[39]
Pool boiling	Novec 7100 (C4F9OCH3)	Parabolic flight	A cell composed of a polycarbonate structure and stainless steel plates, featuring a platinum heater measuring 15 x 15 mm and an electrode positioned 1.6 mm above the heater	The integration of Electrohydrodynamic (EHD) and Dielectrophoretic (DEP) forces enhances the critical heat flux and ensures stable boiling in microgravity, achieving performance comparable to results under Earth's gravity	[40]
Pool boiling	FC-72	Drop tower	A metal foam measuring 5 mm in thickness, 20 mm in diameter, and containing 50 pores per inch	the diameter of bubble departure increases while the departure frequency decreases.	[41]
Pool boiling	Water	ISS	Quartz cell: 10 mm × 20 mm × 43.75 mm; Cu substrates with microstructures of 100–500 nm	In microgravity, the nucleation and growth of bubbles occur up to 30 times faster. Surfaces with finer microstructures can delay the onset of bubble nucleation	[42]
Pool boiling	FC-72	Parabolic flight	Stainless steel cell equipped with a barium fluoride substrate and an "L"-shaped nucleation site (30 μm in diameter and 200 μm in depth)	Preheating duration impacts bubble growth, leading to increased growth rates as the preheating time is extended	[43]
Pool boiling	FC-72	ISS	The boiling cell featured an electrode with voltages of up to 5 kV. Bubble nucleation occurred on a substrate heated by a laser pulse	The electric field caused bubble distortion. The electric field controlled the regular detachment of the bubbles,	[44,45]
Pool boiling	FC-72	Drop tower	Two silicon chips of varying sizes (20 mm × 20 mm × 0.5 mm and 10 mm × 10 mm × 0.5 mm) were heated within a polycarbonate cell	Create a model that incorporates the advancing contact angle and bubble asymmetry, accurately predicting the experimental radius with a deviation of ± 3.8 %	[46]
Pool boiling	FC-72	Drop tower	Polycarbonate chamber containing a smooth silicon chip	Thermocapillary convection ensures bubble attachment at lower heat fluxes; however, at higher flux levels, coalescence causes the bubbles to detach	[47]
Flow boiling	Propane	Vacuum chamber	A system consisting of a mechanical pump, an accumulator, a preheater, a heat exchanger, various heat sources, and condensers	Capillary structures provide efficient fluid management, with the operating point being adjustable through the use of an accumulator	[48]
Flow boiling	FC-72 and Ethanol	Drop tower	Glass tubes varying in diameter from 2.5 mm to 8 mm, featuring flow oscillations that are mechanically induced	Forecasting bubble break-up and coalescence dynamics using the Reynolds number as a key parameter	[49]
Flow boiling	perfluorohexano C6F14	Parabolic flight	A 4 mm aluminum tube with upward vertical flow, tested under microgravity, hypergravity, and normal gravity conditions	There were no substantial variations in heat transfer at elevated mass flow rates	[50]
Flow boiling	n-Perfluorohexano	Parabolic flight	Rectangular channel (2.5 mm × 5.0 mm). Experiments were performed in different orientations under 0 g and 1 g	A novel correlation has been developed to predict the critical flow point under microgravity conditions	[51]
Flow boiling	n-perfluorohexane	ISS	3D gallium heat sink enclosed in a metal casing, paired with a 10x10 cm radiator	Anomalies between Earth and microgravity conditions were noted at low mass velocities and high levels of subcooling	[25]
Flow boiling	FC-72	Parabolic flight	A vertical aluminum tube with different mass flow rates and heat flux	Gravitational effects become insignificant for high mass velocities or when the vapor quality is below −0.2.	[52]
Flow boiling	FC-72	ISS	Trapezoidal copper channel with a smaller base of 1 mm and a height of 5 mm	The liquid film remains confined within the channel grooves, and as power increases, the liquid level in the evaporator decreases. On the ISS, substantial heat loss occurs due to avionics air cooling.	[33,53]
Flow boiling	FC-72	ISS	A rectangular channel (5.0 x 2.5 mm) is heated on opposing walls, with varying mass flow rates and heat input	In microgravity, bubble size increases, and flow patterns undergo significant changes. Computational Fluid Dynamics (CFD) predictions closely matched experimental results	[54]
Flow boiling	Ammonia	Satellite SY-9	The MPTL system is equipped with an evaporator featuring 3.0 mm x 2.0 mm flow channels and a cylindrical accumulator containing capillary structures	The heat transfer coefficients measured in orbit were 10 %-29 % lower than those obtained under terrestrial conditions. The system exhibited precise thermal regulation in microgravity.	[55,56]
Heat pipe	Ethanol	Parabolic flight	A flat plate pulsating heat pipe (FPPHP) featuring 14 milled rectangular channels, each with a 3 × 3 mm^2 cross-sectional area, heated from the bottom surface.	Under normal and hypergravity conditions, the FP-PHP operates in an annular flow regime. In microgravity the flow shifts to a slug/plug regime Capillary rewetting had flow instabilities.	[57,58]

(*continued on next page*)

Table 2 (*continued*)

Method	Fluid	Environment tested	Set-up	Key results	Reference
Heat pipe	water/butanol	Parabolic flight	A single trapezoidal copper groove embedded within a semi-transparent test cell.	The liquid film within the groove remains stable, while the liquid content at the evaporator diminishes as the power input rises. Capillary flow is affected by the gravity level	[59]
Heat pipe	FC-72	Parabolic flight	Flat Plate Pulsating Heat Pipes (FPPHP) were designed with varying internal channel diameters	Channels with larger diameters demonstrated improved thermal performance up to a specific threshold. Changes in gravity created changes in the flow regime	[60,61]
Heat pipe	FC-72	Parabolic Flight	Pulsating Heat Pipe (PHP) fabricated from an aluminium alloy tube, 3 mm inner diameter,14 bends and 50 % filling ratio	The simulation accurately captures the transient start-up behavior.	[62]
Heat pipe	perfluorohexane (C6F14)	Sounding Rocket	Pulsating Heat Pipe (PHP) fabricated from an aluminium alloy tube, 3 mm inner diameter,14 bends and 50 % filling ratio	The PHP effectively demonstrated fluid oscillations and heat transfer in microgravity, with best results than the purely conductive mode.	[63]
Heat pipe	Pure pentene	ISS	A wickless heat pipe with an internal cross-section of 3 mm x 3 mm. The heat was applied to one end, while the opposite end was maintained at a lower temperature	In microgravity, the wickless heat pipe exhibits behaviour predominantly governed by interfacial forces. The experiment revealed the occurrence of a rip current phenomenon. As the condenser temperature was lowered, the heat pipe's overall performance declined	[34,64,65]
Heat pipe	Ammonia	Different orientations	Flat-plate evaporator with vapor grooves, a cylindrical compensation chamber (CC) connected via a secondary wick for liquid supply under microgravity	The FLHPs exhibited two distinct startup conditions. The use of auxiliary startup heating mitigated the effects of thermal overshoot	[66]
Heat pipe	Water	ISS	The hybrid-wick VCHP consists of a copper evaporator with a sintered wick, a Monel adiabatic section, and a condenser equipped with a grooved wick.	The working fluid migrated to the reservoir, leading to higher-than-expected temperatures. Several purging attempts were made to restore functionality; however, the device was unable to resume normal operation	[67]
Heat pipe	R1233zde	Parabolic flight	A Capillary Jet Loop consists of a rectangular loop with an internal diameter of 5 mm. It features an evaporator-ejector assembly, equipped with a porous nickel wick and a 2 mm ejector nozzle	At higher power levels (100 W +), it maintains stable operation under both hypergravity and normal gravity conditions. However, in microgravity, it experiences increased pressure and temperature	[68]
Heat pipe	FC-72	Parabolic flight	An annealed aluminium tube with an internal diameter of 3 mm, featuring 14 turns in the evaporator section with a bending radius of 8 mm. The volume filling ratio is 50 %	The start-up of the device is driven purely by thermal induction, without any influence from previous acceleration fields. Additionally, the fluid oscillation frequencies were successfully characterized	[69,70]
VCC	R-134a	Parabolic flight	Test different inserts (stainless steel discs, aluminium shavings, and felt) for preventing liquid flooding	The insertion of the felt tube proved to be the most efficient method for limiting the flow of liquid refrigerant into the compressor inlet	[71]
PCM	n-octadecane paraffin	Parabolic flight	The experiment involved cells filled with solid n-octadecane and an air layer.	Regulated filling led to a more stable Marangoni convection, increasing the melting rate by as much as 150 %. Thermocapillary convection had a notable impact on heat transfer efficiency	[72,73]
PCM	Gallium	Vacuo	A 3D gallium heat sink enclosed within a metallic housing	Enhanced thermal management attributed to gallium's high density, superior thermal conductivity, and substantial latent heat of fusion	[14]

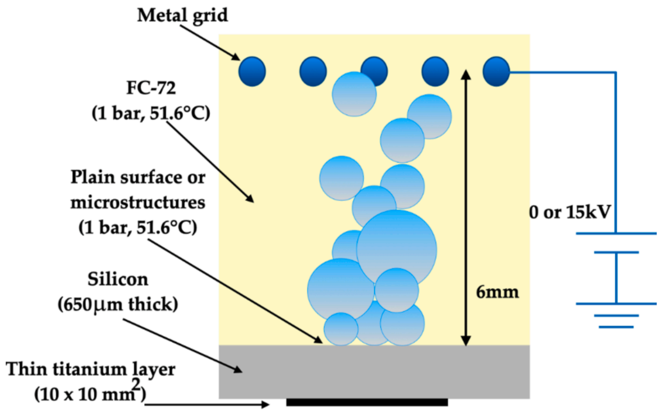

Fig. 2. The conceptual outline of the experiment, consisting of pool boiling in FC-72 fluid that takes place on a heated silicon substrate within an electric field produced by the metal grid,
adapted from [35].

boiling with tests conducted in a drop tower. The findings achieved in a microgravity environment closely resembled those attained under typical gravitational circumstances. The vapor bubbles were slightly larger, but there was minimal coalescence. However, as heat flux increased, bubble size, number, and coalescence all significantly increased. Due to the short duration of microgravity available, steady-state phenomena could not be observed yet.

Zhang et al. [42] conducted a study aiming to better understand the dynamics of nucleation and growth of vapor bubbles on hot surfaces in microgravity, thereby contributing, to a well understanding of fluid-based devices that act in space, such as heat exchangers, mini nuclear reactors, and other applications. The authors observed that nucleation and bubble growth rates can be up to 30 times higher in space than on Earth (Fig. 4) due to the absence of thermal convection that occurs under terrestrial gravity conditions. As there is less heat exchange by convection, heat accumulates in the bubble and in the nucleation centre, allowing growth much greater than that detected in a terrestrial environment.

Shi et al. [41] studied the dynamics of the nucleation and detachment of vapor bubbles using high-speed camera (500 fps) on sponges, and untreated or superhydrophilic surfaces in microgravity. The findings showed that while the departure rate dropped, the bubble diameter grew. The sponge showed a performance up to 86 % better than the surface while being hydrophilic improved the performance by 12 % with a heat removal rate reaching close to 15 W/m^2. The tests were conducted in the drop tower, where the effective microgravity lasts approximately 3.6 s. The experiment utilized a transparent polycarbonate test chamber (120 mmx120 mmx114 mm), a brass test block, and a thermal insulation unit made of polytetrafluoroethylene (PTFE) phenolic plastic and glass wool. FC-72 was used as the working fluid. The authors used type-T thermocouples. The sponge used had a pore density of 50 pores per inch (ppi), a 20 mm diameter and a 5 mm thickness with its surface transformed into superhydrophilic through oxidation. Despite the increase of the heat transfer coefficient when using the hydrophilic sponge, the results compared to the same materials under terrestrial gravity conditions were between 19.2 % and 40 % lower. The reduced performance in microgravity was lower than in Earth's gravity due to the absence of buoyancy forces, which would normally cause the bubbles to move. This led to the creation of a vapor layer that inhibits heat exchange.

In 2018, *Wang* et al. [46] conducted an investigation through experimentation in a drop tower to capture the formation of vapor bubbles using a high-speed camera. The study aimed to better understand the bubble detachment diameter, which currently has limited accuracy in prediction methods. Considering the advancing contact angle instead of the static angle, a revised equilibrium model was proposed with a deviation of only 3.8 % in the conducted experiments.

Nejati et al. [43] performed an experiment to test nucleation from a heat concentration point generated by a laser beam at the center of a glass container aboard an ESA parabolic flight. The objective was to concentrate the nucleation point of vapor bubbles in the middle of the glass by using the laser beam to generate heat. During the experiment, they investigated the influence of preheating on bubble growth and observed that the time of exposure to the laser did not seem to have a significant influence on this aspect.

Vega-Martínez et al. [37] carried out tests to investigate the dynamics of dense bubble cloud formation in supercooled CO2 liquids in microgravity. The experiment was carried out at the Drop Tower of the German Center for Applied Space Technology and Microgravity (ZARM) using an enhanced setup. The formation and growth of the bubble cloud were visualized applying a high-speed camera. The results showed that under microgravity conditions, the bubble cloud continued to grow by diffusion, while under normal gravity conditions, the cloud began to move due to gravity effects. The coalescence of small bubbles was observed during the experiments. A mathematical model was developed to describe the transient growth of a bubble cloud in a supersaturated liquid, considering the diffusion interactions between the bubbles.

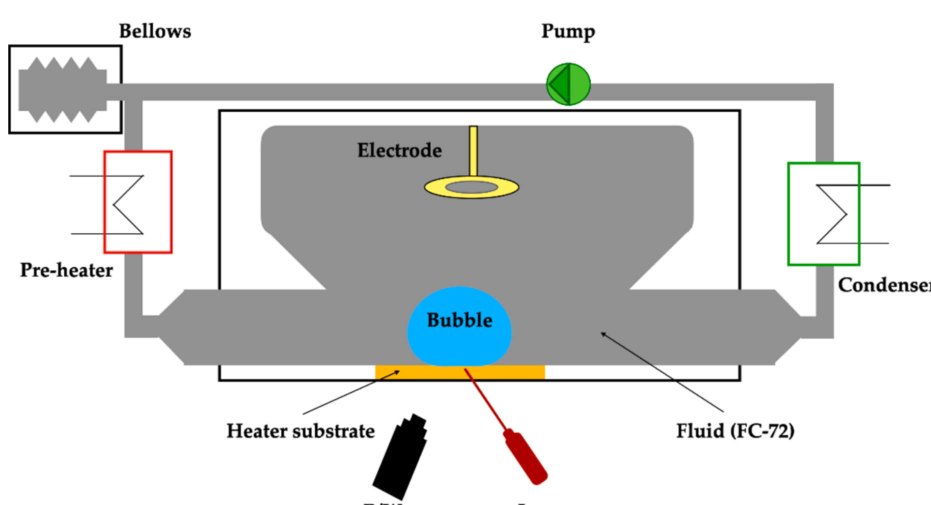

Fig. 3. Boiling cell with its most important components,
adapted from [44].

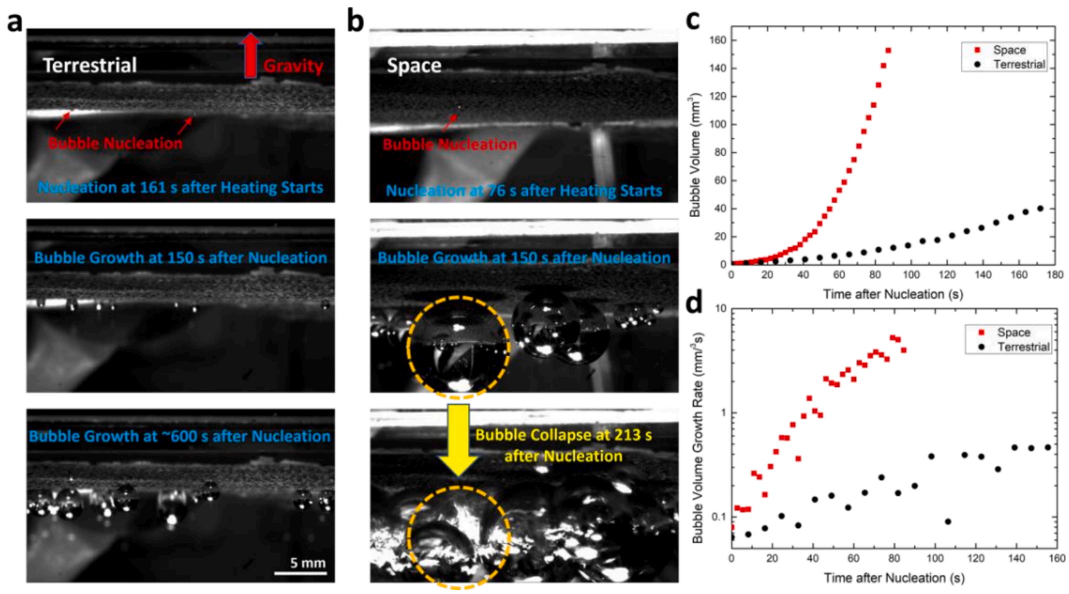

Fig. 4. The visuals depict the emergence of surface bubbles (top), their expansion (middle), and the concluding stage (bottom) in either earthly (a) or microgravity (b) environments. (c) Tracking the evolution of spatial (in red) and earthly (in black) bubbles over time. (d) Graphing the logarithmic growth rates of bubbles over time [42].

2.2. Flow boiling experiments in microgravity

Flow boiling is a phenomenon that occurs in continuous flow systems, such as tubes or channels, where a liquid is warmed above its boiling point. In this process, the liquid undergoes boiling while flowing through the system. The development of vapor bubbles within the liquid is a characteristic of flow boiling, which moves with the flow and transfer thermal energy to the fluid. This phenomenon is extensively studied in heat and mass transfer engineering due to its significance in various applications such as electronics cooling systems, heat exchangers, boilers, and many others. Understanding flow boiling is crucial for designing efficient heat transfer systems and preventing issues like flow instabilities that can occur when excessive vapor formation blocks the liquid flow. Flow boiling is distinguished from pool boiling by the presence of an external pumping mechanism [75].

In their two research studies carried out in 2022, *Meng* et al. [55,56] worked on a thermally controlled accumulator with a passive cooling measure project, using the heat exchange that occurs between the hot liquid in the accumulator and the subcooled liquid from the condenser, called *M*echanically *P*umped *T*wo-phase *L*oop (MPTL) system, as it can be seen in the scheme represented in Fig. 5. This thermal control measure is implemented through a capillary tube, which facilitates heat transfer between the two liquid streams. This approach simplifies the structure of the accumulator compared to traditional models, which often involve the use of thermoelectric (Peltier) elements and other more complex components. The method was tested under low-temperature and vacuum conditions on the ground and in orbit using a satellite. The system demonstrated good performance and stability. The superheat temperature and superheat time parameters were higher in orbit when compared to ground conditions. Tests were conducted with heat sources ranging from 20 to 80 W, gradually increasing the power to observe the fluid behaviour. For pumping, a micro-pump measuring 31x87.5 mm with a flow capacity of up to 2 g/s and a pressure of up to 0.06 MPa was used, operating with Ammonia. The system achieved heat transfer coefficient ranging from 12,000 to 60,000 W/(m^2K), with an efficiency in orbit 12 up to 29 % lower than the results obtained on the ground.

Lee et al. [54] conducted an experiment using a rectangular channel with two opposing heated walls. The channel had dimensions of 5.0 mm (height) x 2.5 mm (width) and a heating zone of 114.6 mm as exhibited

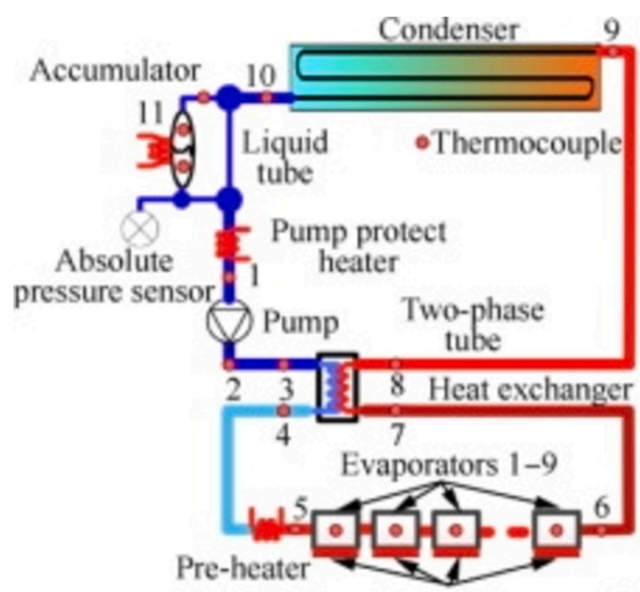

Fig. 5. Scheme of the Mechanically Pumped Two-phase Loop (MPTL) system used by [48].

at Fig. 6. The system was heated by copper resistors. The results were recorded at 2217 frames per second (FPS), using a high-speed camera. The author performed a Computational Fluid Dynamics (CFD) simulation (Fig. 6) based on the Volume of Fluid (VOF) model, which proved effective in both terrestrial and microgravity conditions. The results were validated through parabolic flights where mass flow rate and heat flux were varied, and data such as detailed spatial variation of void fraction, vapor bubbles, mixed fluid temperature, vapor velocity, and liquid velocity were collected. One of the simulation features used to enhance bubble detachment was modelling a shear-lift force, implemented by a user-defined function (UDF). The simulation used the SST k-ω turbulence model, and no modifications to the CFD methodology were required. However, there are some limitations that occur when larger bubbles come into contact, which differs from real-world behaviour and

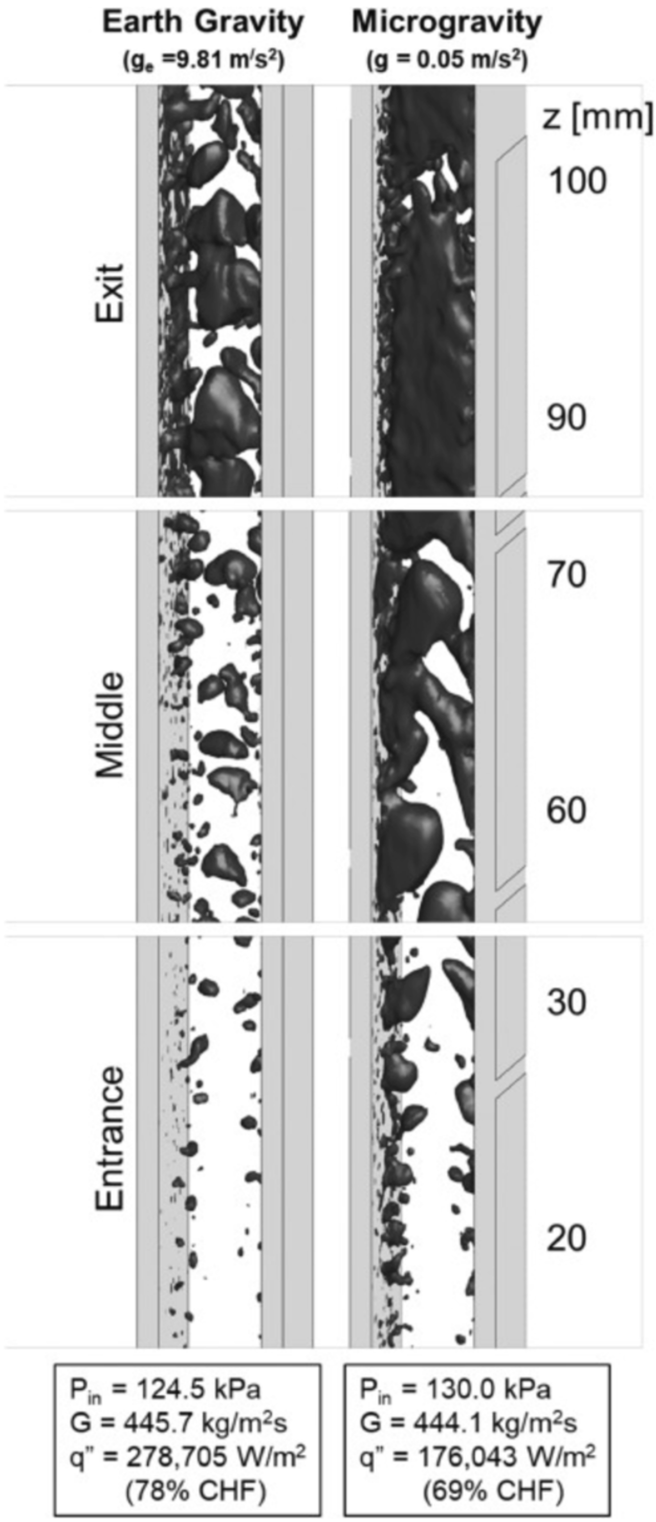

Fig. 6. Calculated biphasic flow structure in vertical upflow in microgravity compared to Earth gravity. Obtained from [54].

makes the simulation less accurate.

Moreover, the authors highlight that, for different flow regimes and their respective variations in nucleation and bubble growth, coalescence, vapor coverage, interfacial ripples, liquid sublayer, the simulation results must be consistent with the experimental observations in all geometry. The work represents a significant advancement since simulations performed for microgravity, based on pressure drop and heat transfer, are conducted using parameters obtained in terrestrial gravity, raising doubts about the validity of such information. However, its application requires a better comprehension of how the fluid, phase change, dynamics and heat transfer mechanisms operate in nearly zero-gravity environments. The simulation results showed that the heat removal capacity is about 35 % lower under microgravity conditions compared to terrestrial conditions. The simulated and measured wall temperatures exhibited an error less than 10 %.

Mudawar et al. [25] conducted experiments aboard the ISS over a period of 5 months to investigate flow boiling in microgravity. Using a high-speed camera, the authors were able to observe the interfacial physical phenomena of the fluids. The tests were conducted in a rectangular channel (2.5 mm x 5.0 mm). A magnetically coupled positive displacement gear pump was utilized to transfer the fluid. The heater operated with electric current, and the condenser consisted of a stainless-steel tube with spiral fins, using water as the working fluid. The fluid pressure was forced by a vent valve and an air pump. The study aimed to evaluate the flow boiling, wall temperature, and heat transfer coefficient as a function of mass flow rate, inlet temperature and pressure.

The conclusions exposed that the fluid flow rate and inlet temperature have a much greater influence than pressure. Additionally, some similarity was observed with tests conducted under terrestrial conditions with vertical upward flow, although the fluid behaviour is quite different, especially when there are instabilities caused by the input parameters. As the heat flux increases, a reduced tendency of wall wetting was observed, resulting in an elevation of the wall temperature above the CHF point. The authors also observed bubble development as the temperature approached CHF, noting that for lower inlet fluid temperatures, the downstream portion of the wall may still remain wet even when the wall temperature reaches CHF.

Iceri et al. [52] used an aluminium cylindrical tube with a diameter of 3.75 mm, with one region insulated by a layer of ceramic fiber. In the experimental study conducted during parabolic flights, the flow was induced by a gear pump, and the heat source was an electric resistance powered by a DC source. The experiment included 9 thermocouples, and the test section had a length of 155 mm. Downstream of the test tube, a transparent tube was used to allow visualization of the phenomenon, using a high-speed camera capable of capturing images at 1000 fps. The condenser was of the shell-tube type, with copper tubes and a polycarbonate shell, and air as the working fluid. The camera captured the initial 2 s of microgravity, following by the final 2 s of hypergravity. The authors demonstrated that existing prediction methods for heat transfer data did not show reasonable agreement and were even unreliable under terrestrial gravity conditions. The researchers also concluded that in microgravity, bubbles are predominantly circular, with elongated bubbles exhibiting circular fronts and flat bottoms, possibly due to the effects of surface tension. Gravity was only found to be significant when the vapor quality reached a certain threshold.

In the experimental study by *Inoue* et al [33,53], the fluid was induced by a circulation gear pump, and the entire system was cooled by the avionics air flow from the ISS. Two tubes were used: one made of glass to observe the fluid behaviour, and another made of metal to study heat transfer. The conclusions showed a substantial heat loss to the environment of the space station, raising an important question for tests conducted in this environment. The vapor quality was evaluated, and a new model was developed to estimate it (Equation (1), showing excellent agreement with empirical data.

$$\frac{\alpha_{TP}}{\alpha_{LO}} = 1 + 15\left(\frac{x}{1-x}\right)^{0.7} \tag{1}$$

where α_{TP} is the heat transfer coefficient (W/m^{2}K) of two-phase fluid; α_{LO} is the heat transfer coefficient (W/m^{2}K) of liquid only, and x is the vapor quality.

Nowak et al. [49] studied oscillatory adiabatic flow in microgravity for channels with Bo > 4 – a parameter that measures the influence of

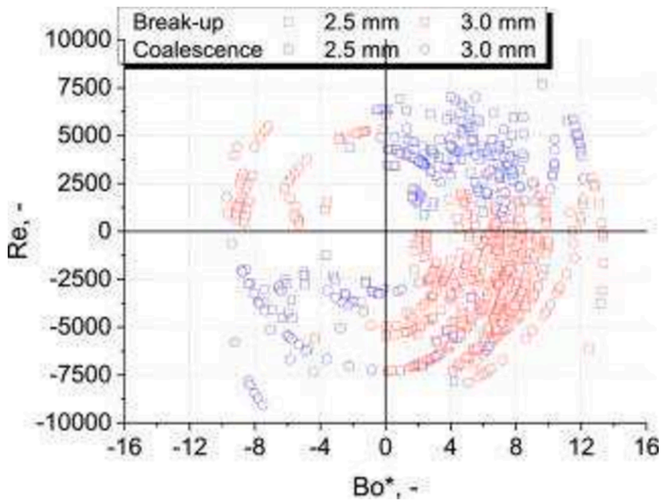

Fig. 8. Map of coalescence and break-up for FC-72—2.5 mm to 3.0 mm diameter. Obtained from [49].

gravity compared to surface tension – in tubes ranging from 2.5 to 8 mm. The flow was mechanically induced to observe the behaviour of bubbles in an adiabatic tube. The work was conducted at the drop tower of the European Space Agency (ESA). The predictability of bubble breakup or coalescence was determined based on the Reynolds number and the modified Bond number (Fig. 8), which has potential application in computational fluid dynamics (CFD).

Darges et al. [51] investigated the CHF of n-Perfluorohexane in a partially heated rectangular channel (2.5 mm x 5.0 mm) within the FBM of the Flow Boiling and Condensation Experiment (FBCE) by NASA. Datasets from previous years' FBM testing in various inclinations under terrestrial gravity (horizontal flow, upward vertical flow, and downward vertical flow) and in parabolic flights were compiled to create a comprehensive CHF-FBCE database, which was then deployed to the ISS. This database encompasses a wide spectrum of operational conditions, including heating configurations (one-side or two-side), distinct gravitational environments, liquid inlets at various sub-coolings, and single-phase saturated inlets at various quality, mass flow rates, and system pressures. The databank was categorized into three types of CHF: subcooled CHF, saturated CHF with single-phase inlet, and saturated CHF with two-phase inlet. The greatest number for the correlations CHF was found by a thorough literature search. This number was then used to generate database-based predictions, and the accuracy of each tiny subset of the predictions was evaluated. While some correlations gave very good predictions for specific subsets of operating conditions, usually those for which they were designed, others were able to produce adequate CHF predictions over broad areas of the database. There was not a single association that could accurately forecast the full database. The gravitational effects on CHF are significant for the various orientations investigated, but many correlations do not take this into account, and even those that do often fail to accurately predict the data in microgravity. To overcome the drawbacks of the current correlations, a new simple CHF correlation is created. This new correlation (Equation (2) was capable to predict the entire consolidated database with a mean absolute error of 17.44 %, showing good agreement for each subset analysed.

$$Bo_{CHF} = q''_{CHF}/(Gh_{fg}) = 0.35We_{D_e}^{-0.314}\left(\frac{L_h}{D_{eq}}\right)^{-0.226}\left(\frac{\rho_f}{\rho_g}\right)^{-0.481}\left(1-\left(\frac{\rho_f}{\rho_g}\right)^{-0.094}x_{e,in}\right)\left(1+0.034\frac{1}{Fr_{\theta,D_e}}\right)\left(1+0.008\frac{Bd_{\theta,D_e}}{We_{D_e}^{0.543}}\right) \tag{2}$$

where Bo_{CHF} is the Boiling number at CHF, q''_{CHF} is critical heat flux, G is the mass velocity, h_{fg} is the latent heat of vaporization; We_{D_e} is Weber number based on channel diameter, L_h is the length, D_{eq} is the equivalent heated diameter, ρ_f is the saturated liquid density, ρ_g is the saturated vapor density, $x_{e,in}$ is the thermodynamic equilibrium quality in channel heated section inlet, orientation-specific Froude number (Fr_θ) is defined as

$$Fr_\theta = \frac{G^2}{\left(\rho_f^2 g\sin\theta D\right)}, \tag{3}$$

where θ is orientation angle of channel, G is the mass velocity and Bd_θ is orientation-specific Bond number defined as

$$Bd_\theta = \frac{g\cos\theta\left(\rho_f-\rho_g\right)D^2}{\sigma}, \tag{4}$$

where σ is the surface tension, g is the gravitational acceleration, and σ the surface tension.

Lancione et al. [50] aimed to analyse heat transfer in two-phase flow under different gravity conditions in an upward vertical flow configuration. The equipment used was an upgraded type of MicroBo (Microgravity Boiling), and the working fluid used was perfluorohexane C6F14. An aluminium channel with a diameter of 4.0 mm was vertically arranged to facilitate the boiling process. The parabolic flight was utilized as the platform to collect the data in microgravity. Two primary methods were used to analyse the data: first, ground-flight data comparison, and second, ground data gathered in the ENEA laboratory using the same configuration were compared. The results demonstrated that there were no significant differences in heat transfer for high mass flow rates (<117 kg/m^{2}s) in earth environment or at microgravity conditions. The authors explain that in microgravity, the relative velocity between the vapor and the liquid is reduced due to the decrease in buoyant force, which also diminishes turbulence at the bubble tails, consequently reducing heat transfer. Increasing the velocity results in a higher relative difference, allowing for greater convective heat exchange.

Bitlloch et al. [38] conducted tests to investigate the formation and behaviour of bubble flows in microgravity conditions. The controlled creation of vapor/liquid bubble circulation by local boiling in zero gravity was successfully proven by the study. The acquired data contributed to a better comprehension of heat transfer events in this form of flow. These findings may have important applications in the development of more efficient cooling systems and the improvement of the performance of space devices operating in microgravity environments.

2.3. Heat pipes experiments in microgravity

Heat pipes are heat exchangers that transfer considerable amounts of heat between the condenser, which is the cool source, and the evaporator, which is the hot source, using a two-phase cycle that does not require external power sources. Capillary action is often utilized in heat pipes to facilitate the movement of the liquid phase, and they are widely employed in cooling chips and microchips both on Earth and in space applications [76].

Slobodeniuk et al. [57,58] found similar Weber numbers for both terrestrial and microgravity conditions in their experiments conducted during a parabolic flight. However, the Garimella number – A dimensionless number used especially in small diameter tubes to characterize boiling. When the value is high, it indicates that surface tension forces have significant relevance in the behavior of the channel; when it is low, it implies that inertial forces have more influence, and the effect of surface tension is less significant-was on average an order of magnitude higher. The experiment involved a molybdenum plate covered with a sapphire window containing 14 rectangular channels measuring 3 mm x 3 mm (Fig. 9). In a similar experimental setup, *Mameli* et al. [69] demonstrated that the initiation of heat pipe operation during the zero-gravity period is possible, and that circulation does not occur solely due to inertia effects, which may still be present when the flow is initiated before the zero-gravity period.

Pagliarini et al. [70] acquired wall temperature data utilizing a high-speed infrared camera and, based on the conclusions obtained, one of the earliest attempts to calculate the heat flow directed toward the walls of such devices under microgravity was made by the author. This allows for acquiring information similar to the one obtained using intrusive instruments or transparent tubes, which can interfere with the original dynamics of the experiments.

Ayel et al. [60] conducted an experiment in parabolic flight with a closed-loop FPPHP with 4 channels filled with FC72 fluid. The experiment took place during ESA's parabolic flight campaigns, with vertical orientations. A thin copper plate was used to build the FPPHP, and on it, a curved channel with eleven U-shaped turns was milled. The top side of the channel was sealed by a transparent borosilicate plate. The authors observed there is a diameter limit beyond which the thermal performance no longer increases, contrary to what is observed under terrestrial gravity conditions. In a similar configuration, it was found that the working fluid exhibited a droplet flow behaviour during microgravity, accompanied by strong temperature oscillations. However, the device still maintained acceptable thermal performance. These results once again highlight the significant influence of channel size and gravity conditions on the flow patterns and heat transfer in the FPPHP [61].

H. Zhang et al. [66] carried out an experiment on a loop heat pipe with a sintered nickel wick, utilizing a stainless steel-ammonia flat-plate configuration. The experiment was performed under terrestrial gravity conditions, with varying orientations. The researchers found that a heating degree above 10 °C is necessary to initiate ammonia boiling when the vapor channels are supplied with liquid. Additionally, they observed that heating the surface near the evaporator outlet is helpful in achieving the needed heating temperature. Another important point is that a secondary wick can be valuable to supply liquid and suppress

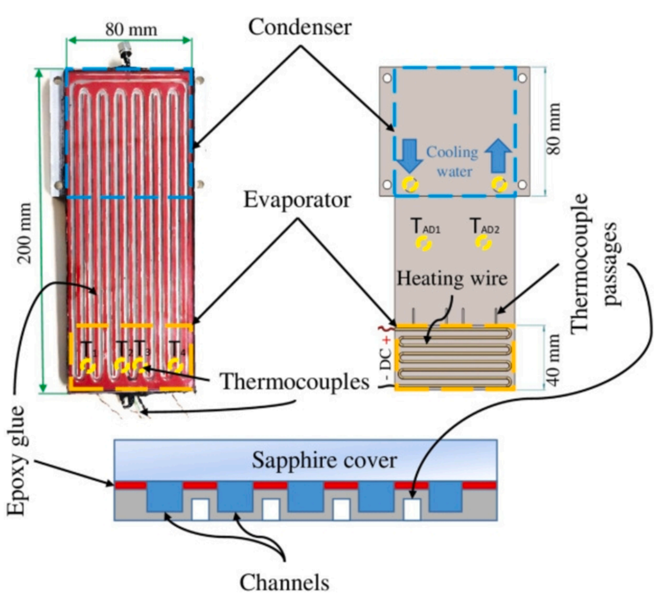

Fig. 9. Setup of the model performed in parabolic flight, tested by [58].

what is sent by the primary wick for use in this type of heat pipe, which is commonly used in space missions. Another observation is that the flat design of the heat pipe, as opposed to a cylindrical one, is advantageous because it allows for more direct contact with the equipment, reducing thermal resistance. The thermal dissipation capability surpassed 330 W, while the critical heat flux was recorded to be in excess of 20 W/cm^2.

Clavenna et al. [68] worked with a mechanism that is a pulsating heat pipe under microgravity conditions and a thermosyphon under gravity or hypergravity conditions. The distinctive feature in this case is a bypass of the capillary jet loop that mixes with the vapor line at the evaporator outlet. Tested in parabolic flight, the device demonstrated its ability to operate in cooling up to 100 W under conditions with acute variations in gravity over short periods of time.

Tarau et al. [67] carried out a test on a hybrid-wick copper-Monel-water variable conductance heat pipe aboard the ISS. In this project, the evaporator was made of copper with a sintered wick and grooved wick in the adiabatic section and condenser. The project was conducted aboard the ISS but encountered higher temperatures than anticipated during testing on Earth. This discrepancy can be attributed to the heat pipe's design, which was not the most suited for microgravity conditions.

Yu et al., [34] in tests conducted aboard the ISS, observed bubble collapse due to increased evaporation. They discovered a relationship between the Ohnesorge number (Oh) –A dimensionless number that links viscous forces to surface and inertial forces. When the value is greater than 1, it indicates the predominance of viscous forces over surface and inertial forces. When it is less than 1, it indicates the predominance of surface and inertial forces- which reflects the fluid viscosity during bubble formation and represents the dissipation of internal viscosity into interfacial tension energy, and the Nusselt number (Nu), as described by Equation (5).

$$Nu = 0.1493[Oh] - 73.7, \tag{5}$$

where Oh is the Ohnesorge number.

In the experiment, a single bubble is formed and tends to position itself in the middle of the heat pipe (Fig. 10). As the system collapses, another bubble is generated, causing the surrounding fluid to move. The energy required for phase change is also extracted from this wall, resulting in cooling [34]. Furthermore, *Yu* et al. [65] found that as the condenser temperature decreases, the performance in microgravity diminishes due to interference of the Marangoni flow. In a study by *Nguyen* et al. [64], the researchers measured the fluid thickness on the wall, the shape and vapor–liquid interface, temperature, and pressure along the heat pipe. In microgravity, Marangoni and capillary forces dominate. When these forces converge, a central droplet is formed, containing two counter-rotating vortices where the highest heat transfer by through evaporation occurs. The role of the return flow in maintaining heat transfer efficiency is crucial as it offers an extra avenue for evaporation near the heater end. Consequently, it can be inferred that the intensity of the return flow is directly proportional to the strength of the Marangoni and capillary flows.

Mameli et al [63] conducted experiments on a wide tube that functions as a thermosyphon loop under normal gravity and transforms into a Pulsating Heat Pipe in microgravity environments. The study was performed on a sounding rocket, which provides a microgravity environment for 120 s, although this duration is insufficient to reach a pseudo-steady state. The tube contained a certain amount of the working fluid, and the condensation section was built by incorporating a PCM within an open-cell metallic foam. The results showed that, during the measured period, the average temperature in the evaporator was significantly lower in microgravity when compared to normal vertical gravity, but higher compared to a 25° inclination. As for the pressure in the condenser, it was higher and exhibited more oscillations in microgravity, with results closer to the 25° inclination than the vertical position.

Abela et al. [62] experimentally validated a 1D simulation of a

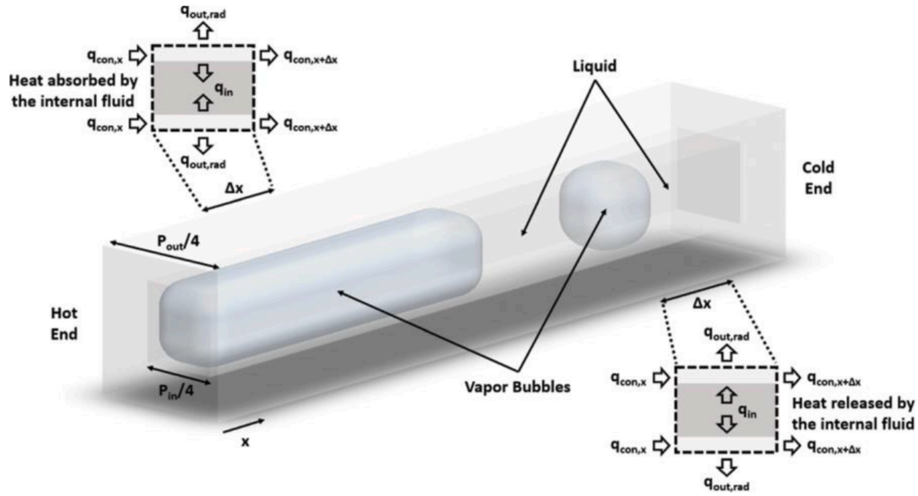

Fig. 10. Schematic of the CVB heat pipe with various heat transfer mechanisms [34].

pulsating heat pipe during parabolic flights. The simulation utilized the CASCo code (French acronym for Code Avancé de Simulation du Caloduc Oscillant: Advanced PHP Simulation Code) to model transient and pseudo-transient regimes, achieving a closely start-up time and an accuracy of 7 % in wall temperatures in different power levels showing an excellent precision with the data evidencing the competence of the technique for the specific case.

Cecere et al. [59] tested a transparent single-groove heat pipe during parabolic flight. The mixture of water and butanol showed more stable behaviour in microgravity due to alterations in surface tension that allows the fluid to keep a liquid film in constant contact with the walls improving the heat transfer.

2.4. Vapor compression cycle (VCC) experiments in microgravity

The vapor compression cycle (Fig. 11) is a highly efficient cycle commonly used for cooling and freezing on Earth, but it is not widely applied in space where the most popular technologies are the reversed Brayton cycle, the Stirling cycle, and thermoelectric cooling [71,77].

The refrigeration cycle encompasses four primary constituents, namely the compressor, condenser, expansion valve, and evaporator. The beginning of this cycle is initiated with the compressor, which assumes the vital role of enhancing the pressure and temperature of the refrigerant. After entering the compressor, the refrigerant is compressed from low-pressure vapor (1) to high-pressure vapor (2). The compressor works on the refrigerant, increasing its energy as the vapor is squeezed. The high-pressure, high-temperature vapor enters the condenser after being compressed. Heat is released from the refrigerant into the surrounding air through the condenser. The refrigerant loses heat and cools down during condensation. The vapor condenses into a high-pressure liquid as a result of the refrigerant releasing heat. The high-pressure liquid refrigerant with reduced temperature (3) then passes through the expansion valve. Because of the adjustable restriction on this valve, liquid refrigerant can enter the evaporator, the following stage, at a significantly lower temperature and pressure (4). The low-pressure liquid refrigerant in the evaporator evaporates and takes up heat from the target cooling environment. The refrigerant changes into a low-pressure, low-temperature vapor as a result of this heat absorption, completing the evaporation process.

An evaluation was conducted on the operation of a vapor compression cycle system, and it was concluded that the fluid charge level has a substantial effect, while the effect of gravity has a lesser impact. This system could be a viable replacement for less efficient Reversed-Brayton cycles. However, there are associated risks with this technology, with the primary concern being the potential for liquid ingress into the air compressor. The objective of the study was to understand the behaviour of phase change. In the study, the authors proposed the use of a "storage tube" in parallel with the evaporator. In this arrangement, another tube would capillary transport the fluid into the storage tube when the system is turned off and gradually release it when turned on, achieving better

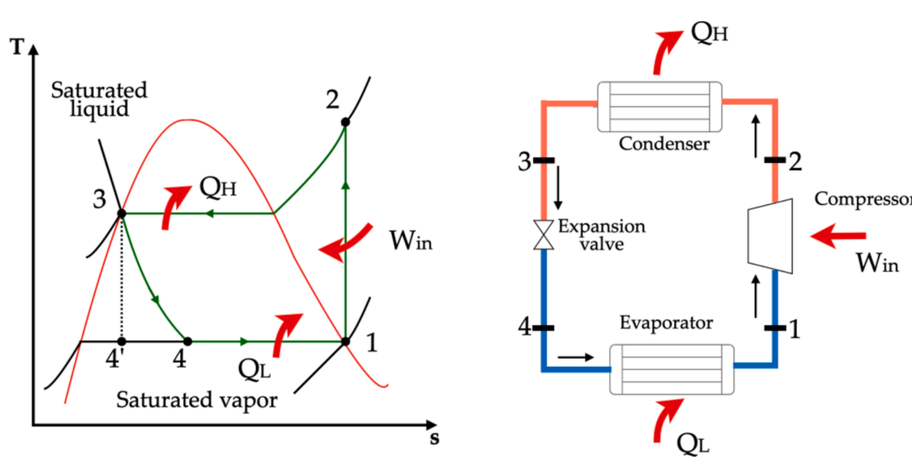

Fig. 11. Ideal Vapor compression cycle, adapted from [78].

Fig. 12. Test samples for tube insertion. Sequentially arranged as: Absence of insertion, stainless steel disc, compressed shavings, and felt, adapted from [71].

results with the use of a wick in the tube (Fig. 12). Another proposed option is to create a temperature difference, resulting in a pressure differential that aids in the fluid transport [71].

2.5. Phase change material (PCM) experiments in microgravity

Phase Change Materials (PCMs) are renowned for their capability to utilize latent heat for heat removal from the surrounding environment, thereby maintaining a controlled temperature at the PCM's melting point. They can also serve as thermal energy storage, preventing temperatures from dropping too low during energy storage. This characteristic proves particularly useful in space applications, especially for electronic components that are not frequently utilized. PCMs, such as paraffin and hydrated salt systems, have been used since the Apollo program. [14,76].

The primary limitations of PCMs are associated with their low thermal conductivity, which becomes the principal factor limiting the heat transfer rate of the material. Additionally, the presence of gravity significantly enhances heat transfer due to the promotion of natural convection. One solution to address these limitations is to increase the contact area with the object being temperature controlled. However, this approach results in increased volume and mass of the system. An alternative method to improve efficiency without increasing mass too much is to incorporate an air layer, as depicted in Fig. 13, which has demonstrated effectiveness in previous simulations. In the first study to use PCM experiments with thermocapillarity in microgravity, the author proposed inducing Marangoni flow through surface tension gradients. One of the focal objectives of the experiment was to observe the conductivity and convection in a microgravity environment with a liquid–air interface. The experiment facilitated increased surface contact area with the melted region and doubled the heat transfer coefficient compared to a fully filled PCM cell [72,73].

In a study similar to the one mentioned earlier, *Sánchez* et al. [79] conducted a numerical modelling using a formulation based on the enthalpy-porosity Navier-Stokes approach. In this investigation, a computational approach rooted in the Finite Element Method (FEM) was employed to simulate various volumes of PCM within the same chamber. The obtained results showed good agreement between the simulated heat transfer and experimental results It is significant to take into account that the results in this study are limited to only a few seconds of simulation. However, this numerical approach provides a valuable tool

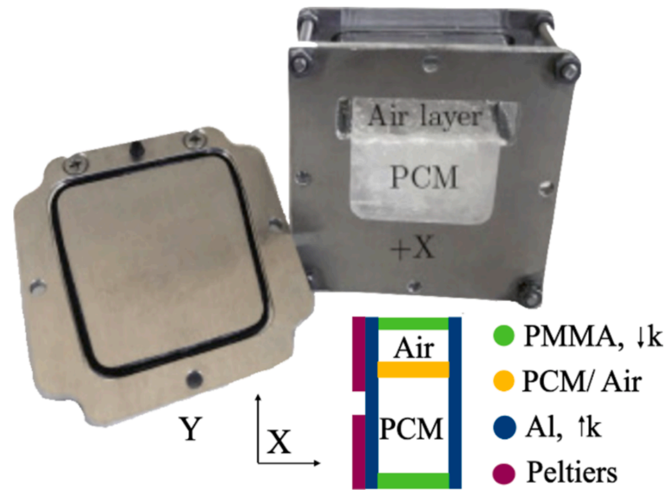

Fig. 13. PCM Cell with an air layer for thermocapillary testing, adapted from [72].

for analysing and understanding heat transfer behaviour in PCM systems in a microgravity environment.

Hartsfield et al. [14] performed a study where gallium was used as the PCM. A gallium cell was specifically designed to establish a connection between a hot surface and the radiator, as illustrated in Fig. 14. The experiment was conducted both under terrestrial conditions and in a vacuum. The usage of gallium as a PCM showed a considerable drop in temperature throughout the phase change process when compared to traditional heat sinks. This reduction can be as high as fifty times, ranging from 1.5 K to 80 K. These finding highlight the effectiveness of gallium as a PCM in heat dissipation, facilitating extremely low temperatures during the phase transition.

3. Nanofluids and new materials for thermal control in space

The advancement of micro and nanochip capabilities, along with the development of electronic devices enabling more accurate measurements of physical parameters, as well as improvements in communication and image capture, leads humanity to significant progress in expanding knowledge beyond Earth. However, this progress introduces new challenges, as it demands the removal of heat in high density, concentrated within very small areas. Moreover, the limitations in space and volume of vehicles designated for space exploration must be considered. In this context, the development of fluids with thermal properties enhancing heat exchange efficiency becomes paramount. Nanofluids, which consist of a base fluid mixed with nanomaterials, have gained prominence in this scenario due to their capacity to enhance the thermal properties of conventional fluids without requiring modifications to existing equipment, and in some cases, even allowing for simplification or reduction in volume [80]. Additionally, the application of nanofluids in a microgravity environment holds significant potential for microgravity applications due to their immunity to sedimentation phenomena, stemming from the density differential between nanoparticles and the surrounding fluid [81]. The use of Polydimethylsiloxane (PDMS), a mouldable material with high flexibility, chemical inertness, corrosion resistance, and low cost, capable of replicating micro-scale geometries, along with its potential for significant wettability variations, and the option for combination with other fibers and particles, should also be considered. This is particularly relevant as PDMS can be transparent, which is essential for studying fluid behavior [82]. Furthermore, PDMS is easily processed without requiring prior training and/or high pressures or temperatures, allowing manufacture the devices locally. Another relevant point is its wide range of applications, from the fabrication of heat exchange devices to medical

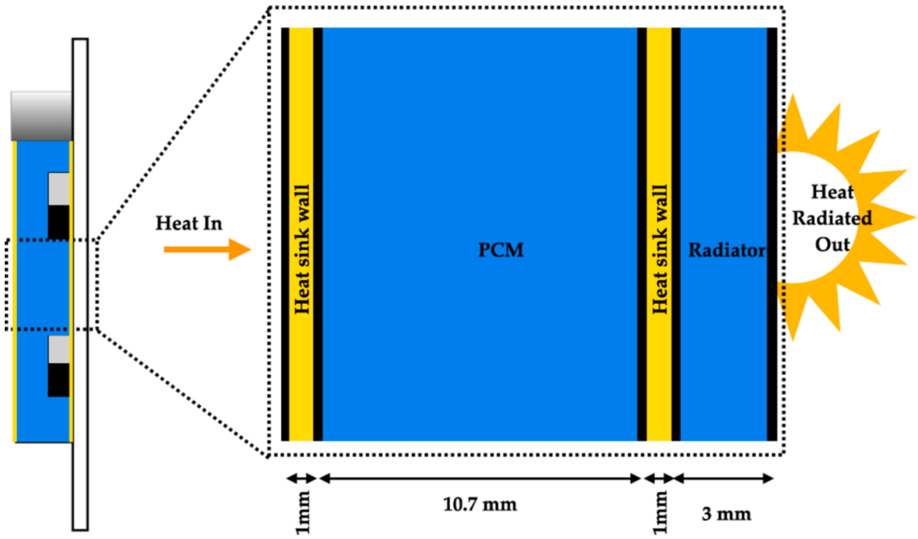

Fig. 14. Configuration of the test assembly performed and adapted by [14].

applications, protective coatings, and electronic uses [83], which enables a reduction in the amount of necessary material, thereby lowering costs.

Under terrestrial conditions, *Freitas* et al. [84] conducted tests and simulations on pool boiling, using various water-based nanofluids with nanoparticles of alumina, aluminum, gold, or silver as the working fluid. The experiments utilized hydrophilic interface surfaces with superhydrophobic regions. The study showcased the potential for greater control over bubble growth, as well as improved efficiency in cooling the surface where the heat source is located. *Tarigonda* et al. [85] performed experiments with hybrid nanofluids consisting of Al_2O_3 and CuO, revealing significant efficiency enhancement in heat pipes. This improvement led to an almost 100 % increase in heat transfer capacity when compared to deionized water, especially in cases of higher input power. *Sarafraz* and *Abad* [86] evaluated the utilization of oil-based carbon nanotube nanofluids. The addition of carbon nanotubes not only enhanced the convective heat transfer coefficient but also increased nucleate boiling in flow boiling experiments. The incorporation of nanoparticles has also found applications in Phase Change Materials (PCMS). In their review, *Eanest Jebasingh* and *Valan Arasu* [87] assessed changes in latent heat and thermal conductivity of PCMS containing nanoparticles within the the range of 20 °C to 37 °C in temperature. The results indicated that the addition of nanoparticles increases thermal conductivity while decreasing latent heat.

Ji et al. [88] designed an oscillating heat pipe made of PDMS that utilized ethanol and an ethanol/Al_2O_3 nanofluid. Interestingly, no significant differences were observed between the use of the nanofluid and pure ethanol. *Mohan* et al. [89] investigated heat transfer in microchannels of PDMS treated with Vacuum Ultraviolet Irradiation. In their work, it was used distilled water and various nanofluids containing nanoparticles of alumina or silica as the base fluids. The results showed that surface effects, whether treated or untreated, were significant only for Reynolds numbers below 10, and that alumina nanofluids yielded the best results.

4. Current status, challenges and the future direction of technology

Addressing the current status of space cooling is a complex task. The fact that space exploration is still predominantly dominated by a limited number of countries, such as the United States, China, Russia, India, Japan, India, France, and Germany, imposes significant constraints on the dissemination of utilized technologies. Due to this, there is a considerable restriction on the disclosure of information. From what has been published, as exemplified by *Gilmore*'s book in 2002 [76], various forms of cooling using two-phase fluids, such as heat pipes, radiators, PCMS, fluid loops, and the combination of these elements, are cited.

Radiators can be mounted on the structural panels of the aircraft, or they can be flat-plate radiators or panels mounted after the spacecraft enters orbit. One of their surfaces is exposed to space, facilitating heat exchange through radiation. It is desirable for this surface to have the highest possible emissivity combined with the lowest absorptance. The most common use of radiators involves integration with an aluminium honeycomb panel that is part of the spacecraft's structure. However, certain applications may require a radiator that is not part of the vehicle's structure. In such cases, the radiator can be either a honeycomb panel or a stiffened aluminium plate, and heat pipes, loop heat pipes, or capillary pumping loops are employed to transfer heat from the equipment to the radiator. Additional heat pipes can also be used to distribute heat across the radiator panel [76].

PCMs have potential use in application in electronic components within launch or re-entry vehicles, capitalizing on its efficiency in managing significant temperature variations over short durations. While the primary application is the temperature control of cyclically operating electronic equipment, it has also been employed in the Lunar Roving Vehicle during the Apollo 15 mission. The utilization of PCMs in celestial bodies lacking an atmosphere proves advantageous due to temperature fluctuations. Furthermore, it is recommended for satellite applications, especially in scenarios where there is a substantial temperature variation during transitions between shadowed and illuminated spaces. Instruments requiring precise calibration are also well-suited for PCM use to ensure temperature stability[76].

Various coolant materials can be employed, with water being a notable example utilized in the Gemini and Apollo missions. Other materials are utilized based on a combination of melting point, specific heat, and thermal conductivity. Among the more important materials are inorganic salt hydrates, organic compounds, eutectics of organic materials, and natural inorganic elements.[76].

Pumped fluid loops comprise a pump device, a heat exchanger, and a radiator typically cooled through radiation exchange with space. Satellites from the USA Defense Program and the ISS utilize this cooling method with ammonia serving as the thermal fluid [76,90]. The selection of the appropriate thermal fluid is crucial and involves evaluating properties such as freezing point, boiling point, specific heat, thermal conductivity, and compatibility with the materials used[76].

Heat pipes are closed two-phase liquid systems composed of an evaporator and a condenser, with liquid transfer facilitated by capillarity. In the telescope tube of NASA's Orbiting Astronomical Observatory, three heat pipes with ammonia were employed to minimize temperature gradients during the eight years of operation [76].

Thermal control of batteries in space is one of the biggest challenges, but one can take advantage of the advances in these areas that have been developed in studies focused on applications in electric cars. This system aims to maintain the temperature of vehicle batteries within a range where they exhibit optimal performance, as the chemical reactions involved are highly temperature dependent. Additionally, batteries have a unique condition where the temperature hotspot is located near the electrode compared to the rest of the battery body and tends to experience temperature variations due to the fluctuation in internal heat generation during both the charging (endothermic) and discharging (exothermic) processes [91].

Within the context of battery technology, PCM (Phase Change Material) emerges as a promising option. PCM is a material capable of storing and releasing energy during phase change, offers significant benefits. One of the main advantages is its ability to manage the heat generated during the battery charging and discharging process[91]. The most extensively studied method involves the use of metal foams, with foams made from copper, aluminium, and nickel being addressed. Another applied technique is the incorporation of carbon-based materials such as graphene, films, nanoplatelets, and nanotubes either in paraffin or within the foam structure[91].

The Jet Propulsion Laboratory, located at the prestigious California Institute of Technology, has effectively exhibited the management of thermal conditions for the batteries of Mars lander and rover, ensuring that temperatures remain within the specific range of −10 °C to + 25 °C. [92]. The utilization of a PCM and a loop heat pipe (LHP) effectively maintained the minimum threshold of the battery temperature. Within this particular system, the PCM thermal storage module functions as a means to both store and release heat, while the LHP effectively transfers heat from a collection of Radioisotope Heater Units to the battery. Furthermore, the upper limit of the battery temperature can be effectively regulated by means of opening a thermal control valve within the LHP, which allows for the management of fluid flow to an external radiator. This radiator serves to release any excess heat into the atmosphere. [93].

The Indian lander Chandrayaan-3. which for the first time touched down the Moon's south pole, couldn't survive for more than few days due to the lunar nightfall. Scientists believe that the cold temperature damaged the equipment [94]. This situation demonstrated that the concern cannot be just about the heat removed but also about keeping the heat when it's necessary. One option is the Jumping-Drop Thermal Diode tool transports heat through a two-phase cycle, as well as heat pipe exchangers and other types of technologies that utilize this technique. The operation is as follows: the condenser is coated with a superhydrophobic material that causes the condensed drops to come off without the action of external forces, while the evaporator is a tank of porous super hydrophilic material with a gap vacuum between the two surfaces. Its operation basically occurs through latent heat transfer as follows: The smaller droplets that are generated in the condenser end up getting together with the surrounding drops until they are large enough for the surface tension force to make the drop break free from the superhydrophobic surface of the condenser [95,96] In the reverse direction, the cycle only occurs via steam, and since the distance between the evaporator and condenser is only a few millimetres, there is minimal heat exchange by convection.

In this context, noteworthy techniques enable the creation of superhydrophilic and superhydrophobic surfaces, holding significant potential for applications, particularly in the realm of heat exchange through boiling. Lithography techniques have assumed a prominent role, allowing for the manipulation of nano or microstructured surfaces. In addition to the material used, the design plays a crucial role in influencing this parameter. Typically, on a plate, the printed area exhibits hydrophobic characteristics, while the non-printed area tends to be more hydrophilic. This is exemplified in the work of *Tian* et al. [97], where numerous instances are presented wherein superhydrophobic structures and materials are printed alongside hydrophilic structures. *Oliveira* et al. [98] conducted research on phase change on polystyrene surfaces using phase separation and UV/Ozone radiation. The study enabled the alteration of surface wettability, ranging from angles close to 0° to superhydrophobic surfaces with angles greater than 151°. *Ul Hassan* et al. [99] confirmed that alterations in wettability impact the speed of fluid penetration between two parallel plates. Hydrophilic and superhydrophilic surfaces demonstrated a greater capacity to spread the fluid compared to hydrophobic surfaces. The study also revealed that the presence of electric fields influences fluid penetration in all scenarios. The control of surface wettability enables enhanced management of critical heat flow points, the locations of bubble formation and growth, and has a direct impact on surface capillarity. This characteristic can be harnessed for pumping in heat pipes and extending the distance between condensers and evaporators. Consequently, it grants greater flexibility in the design of spacecraft.

Although advances have been made recently, CFD simulation methods are still imprecise in relation to phase changes, especially in a microgravity environment, therefore the use of other simulation technologies such as Molecular Dynamics (MD) can offer more reliable results and offer better insights into the phenomena of two-phase transitions. Several simulations have been conducted to gain a better understanding of fluid behaviour in microgravity conditions [100].

Chen and Tong [100], for instance, explored the wettability of water on a gold surface with a face-centred cubic structure in microgravity using the *LAMMPS* software. In Earth gravity, *Lie* et al. investigated the effects of changes in surface wettability on the thermal and atomic behaviour of ammonia/copper nanofluids. They observed that the presence of a hydrophilic surface increased the thermal conductivity of nanofluids [101]. *Liu* et al. [102] simulated the effects of copper oxide nanoparticles in PCM, focusing on phase change transitions and demonstrating changes even in the duration of transitions. Additionally, *Jarmatz* et al. [103] developed software that enables simultaneous work with CFD and MD in parallel on a supercomputer, allowing for simulations in a multiscale context.

While Molecular Dynamics (MD) can offer new insights into heat transfer phenomena in microgravity conditions, it comes with certain challenges. The computational cost is a significant concern due to the high number of particles involved, which imposes limitations on the domain size and simulation time. Additionally, accurately inputting the energy of the system and modeling the interactions between particles pose difficulties. These challenges underscore the need for careful consideration and validation when employing MD simulations for studying heat transfer in microgravity environments [103].

5. Conclusions

This review describes the most recent cooling methods involving in two-phase fluid experiments performed in microgravity environment. Based on the findings of this article, the following conclusions can be drawn:

- Conducting two-phase cooling tests in microgravity conditions results in a lower performance when compared to tests conducted on Earth. The absence of buoyancy forces affects other properties such as surface tension, resulting in a lower performance. Hence, it is essential to perform further fluid experiments in microgravity conditions to gain a better understanding of these phenomena, despite the limitations and costs involved;
- Although there have been advancements in fluid modelling, capable of providing more accurate results, there is still a margin of error of around 20 % or even higher. Simulations in terrestrial gravity conditions are already challenging and become even more complex in

the absence of buoyancy forces. CFD simulations are reliable for single-phase regimes but face difficulties in accurately simulating multiphase flows even under gravity conditions present on Earth's surface;
- The use of electric fields shows promising advancements as it can enhance heat transfer efficiency and provide greater predictability of fluid behaviour. However, implementing these methods, especially in space, remains challenging, and the tests conducted used potential differences that are not feasible in long-term heat exchangers;
- There is a crucial need to better understand phase change phenomena in space. With increased access to space by new players such as China, India, Japan, and private companies, there are future prospects for advancements in this area;
- Most studies investigate only a single fluid, limiting the ability to extrapolate the results, even when the models agree well with experimental findings;
- The combination of different heat exchangers, especially with phase change materials (PCMs), demonstrates significant potential for application, as well as alterations in surface wettability;
- Tests conducted at specific inclinations can be a viable alternative, at least for preliminary studies, considering that microgravity tests are expensive, have significant limitations, and have limited availability.
- Nanofluids possess significant potential for space applications due to their enhanced thermal properties, which are particularly advantageous in the nearly gravity-free environment. Nevertheless, nanoparticle agglomeration remains a concern. Transparent heat exchanger tests, such as those conducted using PDMS, can offer a means not only to produce more efficient heat exchangers but also to observe phenomena occurring during the heat exchange process. This has the potential to yield insights into how nanofluids perform in such conditions, contributing to advancements in space-based thermal management systems.

CRediT authorship contribution statement

Glauco Nobrega: Writing – review & editing, Writing – original draft, Methodology, Conceptualization. **Inês Santos Afonso:** Writing – review & editing, Writing – original draft, Conceptualization. **Beatriz Cardoso:** Writing – review & editing, Writing – original draft, Validation, Data curation. **Reinaldo Rodrigues de Souza:** Writing – original draft, Validation, Supervision, Funding acquisition, Conceptualization. **Ana Moita:** Writing – review & editing, Validation, Supervision, Resources, Funding acquisition. **João Eduardo Ribeiro:** Writing – review & editing, Validation, Supervision, Funding acquisition. **Rui A. Lima:** Writing – review & editing, Validation, Supervision, Resources, Funding acquisition.

Declaration of competing interest

The authors declare that they have no known competing financial interests or personal relationships that could have appeared to influence the work reported in this paper.

Acknowledgements

Authors acknowledge to Fundação da Ciência e da Tecnologia (FCT), for partially funding this research through project PTDC/EME-TED/7801/ 2020, and by LA/P/0083/2020 IN +, UIDP/50009/2020-FCT and UIDB/50009/2020, UIDB/04077/2020, UIDP/04077/2020, UIDB/00532/2020, LA/P/0045/2020 (ALiCE), CIMO (UIDB/00690/2020) and SusTEC (LA/P/0007/2020), and 2022.03151.PTD (https://doi.org/10.54499/2022.03151.PTDC). G. Nobrega was supported by the doctoral PRT/BD/153088/2021, financed by the Portuguese Foundation for Science and Technology (FCT), and with funds from MCTES/República Portuguesa, under MIT Portugal Program. I. Afonso was supported by the doctoral 2024.05919.BDANA, financed by the Portuguese Foundation for Science and Technology (FCT). A.S. Moita also acknowledges FCT for partially financing her contract through CEECINST/00043/2021/CP2797/CT0005, doi: 10.54499/CEECINST/00043/2021/CP2797/CT0005.

Data availability

Data will be made available on request.

References

[1] P.I.Y. Velinov, Development of Advanced Space Sciences after First Artificial Satellite. 60-Th Anniversary ff the Space Age. Bulgarian, Acad. Sci. 29 (2017) 147–157.
[2] NASA. Sputnik 2 n.d. https://nssdc.gsfc.nasa.gov/nmc/spacecraft/display.action?id=1957-002A (accessed April 13, 2023).
[3] Hibbs AR. Explorer1/ResistanceThermometers n.d. https://nssdc.gsfc.nasa.gov/nmc/experiment/display.action?id=1958-001A-04 (accessed June 26, 2023).
[4] G. Heller, Thermal Control of the Explorer Satellites, ARS Journal 30 (1960) 344–352, https://doi.org/10.2514/8.5071.
[5] N. Moiseev, Life Support Systems for Russian IVA/EVA Space Suits. Handbook of Life Support Systems for Spacecraft and Extraterrestrial Habitats, Springer International Publishing (2016) 1–20, https://doi.org/10.1007/978-3-319-09575-2_5-1.
[6] Williamson M. Technology of Vostok One 2011. https://eandt.theiet.org/content/articles/2011/03/technology-of-vostok-one/ (accessed April 20, 2023).
[7] L.P.M. Brendel, S.L. Caskey, M.K. Ewert, D. Hengeveld, J.E. Braun, E.A. Groll, Review of vapor compression refrigeration in microgravity environments, Int. J. Refrig 123 (2021) 169–179, https://doi.org/10.1016/j.ijrefrig.2020.10.006.
[8] Karam RD. Satellite Thermal Control for Systems Engineers. vol. 181. American Institute of Aeronautics and Astronautics, Inc; 1998.
[9] S.M. Bruno, The Geopolitical Implications of Commercialization of Satellite Technology. Sandia National Lab, (SNL-NM), Albuquerque, NM (united States) (2021).
[10] J. Miao, Q. Zhong, Q. Zhao, X. Zhao, Spacecraft Thermal Control Technologies, Singapore: Springer Singapore (2021), https://doi.org/10.1007/978-981-15-4984-7.
[11] Z. Du, M. Li, S. Xu, K. Li, F. Zou, R. Zhang, et al., VO2-based intelligent thermal control coating for spacecraft by regulating infrared emittance, J. Alloy. Compd. 895 (2022) 162679, https://doi.org/10.1016/j.jallcom.2021.162679.
[12] B. Yost, S. Weston, State-of-the-Art Small Spacecraft Technology, Hanover, Maryland, USA, 2021.
[13] D. Xu, J. Zhao, L. Liu, Near-field radiation assisted smart skin for spacecraft thermal control, Int. J. Therm. Sci. 165 (2021) 106934, https://doi.org/10.1016/j.ijthermalsci.2021.106934.
[14] C.R. Hartsfield, T.E. Shelton, B.O. Palmer, R. O'Hara, All-Metallic Phase Change Thermal Management Systems for Transient Spacecraft Loads, J. Aerosp. Eng. 33 (2020), https://doi.org/10.1061/(ASCE)AS.1943-5525.0001150.
[15] Johnston RS, Dietlein LF. Biomedical Results from Skylab. 1977.
[16] Seedhouse E. Life Support Systems for Humans in Space. 2020. https://doi.org/https://doi.org/10.1007/978-3-030-52859-1.
[17] W. Hu, Q. Kang, Physical Science Under Microgravity: Experiments on Board the SJ-10 Recoverable Satellite, Singapore: Springer Singapore (2019), https://doi.org/10.1007/978-981-13-1340-0.
[18] H.M. Ali, Applications of combined/hybrid use of heat pipe and phase change materials in energy storage and cooling systems: A recent review, J Energy Storage 26 (2019) 100986, https://doi.org/10.1016/j.est.2019.100986.
[19] A. Sielaff, D. Mangini, O. Kabov, M.Q. Raza, A.I. Garivalis, M. Zupančič, et al., The multiscale boiling investigation on-board the International Space Station: An overview, Appl. Therm. Eng. 205 (2022) 117932, https://doi.org/10.1016/j.applthermaleng.2021.117932.
[20] J.-X. Wang, W. Guo, K. Xiong, S.-N. Wang, Review of aerospace-oriented spray cooling technology, Prog. Aerosp. Sci. 116 (2020) 100635, https://doi.org/10.1016/j.paerosci.2020.100635.
[21] R. Liu, L. Zhang, X. Zhang, Applications of Spray Cooling Technology in Aerospace Field, IOP Conf. Ser.: Mater. Sci. Eng. 470 (2019) 012020, https://doi.org/10.1088/1757-899X/470/1/012020.
[22] M.M. Weislogel, J.C. Graf, A.P. Wollman, C.C. Turner, K.J.T. Cardin, L.J. Torres, et al., How advances in low-g plumbing enable space exploration, Npj Microgravity 8 (2022), https://doi.org/10.1038/s41526-022-00201-y.
[23] C. Konishi, I. Mudawar, Review of flow boiling and critical heat flux in microgravity, Int. J. Heat Mass Transf. 80 (2015) 469–493, https://doi.org/10.1016/j.ijheatmasstransfer.2014.09.017.
[24] S. Hong, J. Wang, Z. Gao, C. Dang, Review on state-of-the-art research in pool and flow boiling under microgravity, Exp. Therm Fluid Sci. 144 (2023) 110848, https://doi.org/10.1016/j.expthermflusci.2023.110848.
[25] I. Mudawar, V.S. Devahdhanush, S.J. Darges, M.M. Hasan, H.K. Nahra, R. Balasubramaniam, et al., Heat transfer and interfacial flow physics of microgravity flow boiling in single-side-heated rectangular channel with subcooled inlet conditions – Experiments onboard the International Space Station, Int. J. Heat Mass Transf. 207 (2023) 123998, https://doi.org/10.1016/j.ijheatmasstransfer.2023.123998.

[26] L.P. Brendel, J.A. Weibel, J.E. Braun, E.A. Groll, Microgravity two-phase flow research in the context of vapor compression cycle experiments on parabolic flights, Int. J. Multiph. Flow 160 (2023) 104358, https://doi.org/10.1016/j.ijmultiphaseflow.2022.104358.
[27] K. Sridhar, R. Smith, V. Narayanan, S. Bhavnani, Phase Change Cooling of Spacecraft Electronics: Terrestrial Reference Experiments Prior to ISS Microgravity Experiments, in: 2020 19th IEEE Intersociety Conference on Thermal and Thermomechanical Phenomena in Electronic Systems (ITherm), IEEE, 2020, pp. 315–322, https://doi.org/10.1109/ITherm45881.2020.9190438.
[28] R.R. Souza, V. Faustino, J.D. Oliveira, I.M. Gonçalves, J.M. Miranda, A.S. Moita, et al., A novel and extremely stable nanofluid based on iron oxide nanoparticles: Experimental investigations on the thermal performance, Therm. Sci. Eng. Prog. 26 (2021) 101085, https://doi.org/10.1016/j.tsep.2021.101085.
[29] L.P.M. Brendel, J.E. Braun, E.A. Groll, Matching Testing Possibilities and Needed Experiments for Successful Vapor Compression Cycles in Microgravity, MATEC Web of Conferences 324 (2020) 02001, https://doi.org/10.1051/matecconf/202032402001.
[30] L. Luo, H. Zhou, Y. Sun, W. Zhang, T. Chen, S. Chen, et al., Tsinghua University Freefall Facility (TUFF): A 2.2 Second Drop Tunnel for Microgravity Research. Microgravity, Sci. Technol. 33 (2021) 26, https://doi.org/10.1007/s12217-021-09877-5.
[31] E. Gibney, How to build a Moon base, Nature 562 (2018) 474–478, https://doi.org/10.1038/d41586-018-07107-4.
[32] B. Liu, B. Yuan, P. Xu, J. Zhao, Y. Zhang, J. Wei, et al., A method for approximating the CHF of subcooled flow boiling in microgravity by ground tests, Int. J. Multiph. Flow 122 (2020) 103161, https://doi.org/10.1016/j.ijmultiphaseflow.2019.103161.
[33] K. Inoue, H. Ohta, Y. Toyoshima, H. Asano, O. Kawanami, R. Imai, et al., Heat Loss Analysis of Flow Boiling Experiments Onboard International Space Station with Unclear Thermal Environmental Conditions (1st Report: Subcooled Liquid Flow Conditions at Test Section Inlet), Microgravity Sci. Technol. 33 (2021) 28, https://doi.org/10.1007/s12217-021-09869-5.
[34] J. Yu, A. Pawar, J.L. Plawsky, D.F. Chao, The effect of bubble nucleation on the performance of a wickless heat pipe in microgravity, Npj Microgravity 8 (2022) 12, https://doi.org/10.1038/s41526-022-00197-5.
[35] A.I. Garivalis, G. Manfredini, G. Saccone, P. Di Marco, A. Kossolapov, M. Bucci, Critical heat flux enhancement in microgravity conditions coupling microstructured surfaces and electrostatic field, Npj Microgravity 7 (2021) 37, https://doi.org/10.1038/s41526-021-00167-3.
[36] G. Saccone, A.I. Garivalis, P. Di Marco, Electrohydrodynamics and boiling: Experiments, numerical calculation and modeling of Maxwell stress tensor and electric force acting on bubbles, J. Electrostat. 103 (2020) 103413, https://doi.org/10.1016/j.elstat.2019.103413.
[37] P. Vega-Martínez, J. Rodríguez-Rodríguez, D. van der Meer, Growth of a bubble cloud in CO2-saturated water under microgravity, Soft Matter 16 (2020) 4728–4738, https://doi.org/10.1039/D0SM00015A.
[38] P. Bitlloch, X. Ruiz, L. Ramírez-Piscina, J. Casademunt, Controlled Generation of Vapor/Liquid Slug Flows by Local Boiling in Microgravity, AIAA J. 58 (2020) 4017–4027, https://doi.org/10.2514/1.J058619.
[39] Á. Romero-Calvo, Ö. Akay, H. Schaub, K. Brinkert, Magnetic phase separation in microgravity, Npj Microgravity 8 (2022) 32, https://doi.org/10.1038/s41526-022-00212-9.
[40] A.J. Castaneda, N.J. O'Connor, J.S. Yagoobi, J.R. Didion, M.S. Martins, M. M. Hasan, Dielectrophoretically-Assisted Electrohydrodynamic-Driven Liquid Film Flow Boiling in the Presence and Absence of Gravity. ASME Journal of, Heat Mass Transf. 145 (2023), https://doi.org/10.1115/1.4055566.
[41] J. Shi, D. Feng, Z. Chen, Experimental investigation on pool boiling heat transfer on untreated/super-hydrophilic metal foam under microgravity, Int. J. Heat Mass Transf. 151 (2020) 119289, https://doi.org/10.1016/j.ijheatmasstransfer.2019.119289.
[42] Q. Zhang, D. Mo, J. Janowitz, D. Ringle, D. Mays, A. Diddle, et al., Bubble Nucleation and Growth on Microstructure Surface under Microgravity, ArXiv Preprint ArXiv:2304 (2023), https://doi.org/10.48550/arXiv.2304.02717.
[43] I. Nejati, A. Sielaff, B. Franz, M. Zimmermann, P. Hänichen, K. Schweikert, et al., Experimental Investigation of Single Bubble Nucleate Boiling in Microgravity, Microgravity Sci. Technol. 32 (2020) 597–607, https://doi.org/10.1007/s12217-020-09813-z.
[44] A.I. Garivalis, P. Di Marco, Isolated bubbles growing and detaching within an electric field in microgravity, Appl. Therm. Eng. 212 (2022) 118538, https://doi.org/10.1016/j.applthermaleng.2022.118538.
[45] M. Bucci, M. Zupančič, A.I. Garivalis, A. Sielaff, P. Di Marco, I. Golobič, The role of the electric field in the departure of vapor bubbles in microgravity, Phys. Fluids 35 (2023) 017109, https://doi.org/10.1063/5.0127123.
[46] X. Wang, Z. Wu, J. Wei, B. Sunden, Investigation of Bubble Departure Radius in Subcooled Pool Boiling Under Microgravity Condition. Volume 8A: Heat Transfer and Thermal Engineering, Am. Soc. Mech. Eng. (2018), https://doi.org/10.1115/IMECE2018-87741.
[47] Y.-F. Xue, J.-F. Zhao, J.-J. Wei, J. Li, D. Guo, S.-X. Wan, Experimental Study of Nucleate Pool Boiling of FC-72 on Smooth Surface under Microgravity, Microgravity Sci. Technol. 23 (2011) 75–85, https://doi.org/10.1007/s12217-011-9274-5.
[48] Q. Meng, T. Zhang, F. Yu, Y. Zhao, Z. Zhao, Z. Zhou, Experimental study on dynamic behavior of mechanically pumped two-phase loop with a novel accumulator in simulated space environment, Chin. J. Aeronaut. 35 (2022) 102–116, https://doi.org/10.1016/j.cja.2022.06.004.
[49] A.I. Nowak, L. Pietrasanta, C. Czajkowski, M. Marengo, S. Pietrowicz, Bubble coalescence and break-up in confined oscillating two-phase flows under microgravity conditions, Int. J. Heat Mass Transf. 192 (2022) 122905, https://doi.org/10.1016/j.ijheatmasstransfer.2022.122905.
[50] G. Lancione, D. Mieko Iceri, L. Gugliermetti, L. Saraceno, G. Zummo, F. Bisegna, et al., Two-Phase Heat Transfer in 4.0 mm Tube Under Different Gravity Conditions, J. Phys. Conf. Ser. 1599 (2020) 012009, https://doi.org/10.1088/1742-6596/1599/1/012009.
[51] S.J. Darges, V.S. Devahdhanush, I. Mudawar, Assessment and development of flow boiling critical heat flux correlations for partially heated rectangular channels in different gravitational environments, Int. J. Heat Mass Transf. 196 (2022) 123291, https://doi.org/10.1016/j.ijheatmasstransfer.2022.123291.
[52] D.M. Iceri, G. Zummo, L. Saraceno, G. Ribatski, Convective boiling heat transfer under microgravity and hypergravity conditions, Int. J. Heat Mass Transf. 153 (2020) 119614, https://doi.org/10.1016/j.ijheatmasstransfer.2020.119614.
[53] K. Inoue, H. Ohta, H. Asano, O. Kawanami, R. Imai, K. Suzuki, et al., Heat Loss Analysis of Flow Boiling Experiments Onboard International Space Station with Unclear Thermal Environmental Conditions (2nd Report: Liquid-vapor Two-phase Flow Conditions at Test Section Inlet), Microgravity Sci. Technol. 33 (2021) 57, https://doi.org/10.1007/s12217-021-09902-7.
[54] J. Lee, I. Mudawar, M.M. Hasan, H.K. Nahra, J.R. Mackey, Experimental and computational investigation of flow boiling in microgravity, Int. J. Heat Mass Transf. 183 (2022) 122237, https://doi.org/10.1016/j.ijheatmasstransfer.2021.122237.
[55] Q. Meng, Z. Zhao, X. Chen, Ground Test and on-Orbit Verification of a Mechanically Pumped Two-Phase Loop Using for Thermal Control of Spacecraft, Heat Transfer Eng. (2022) 1–19, https://doi.org/10.1080/01457632.2022.2140629.
[56] Q. Meng, F. Yu, Y. Zhao, Z. Zhao, On-orbit Test and Analyses of Operating Performances for Mechanically Pumped Two-phase Loop in Microgravity Environment, Microgravity Sci. Technol. 34 (2022) 45, https://doi.org/10.1007/s12217-022-09966-z.
[57] Slobodeniuk M, Ayel V, Bertossi R, Romestant C, Miché N, Bertin Y, et al. Experimental analysis of the fluid flow in the flat plate pulsating heat pipe under microgravity conditions. International Symposium on Oscillating/Pulsating Heat Pipes (ISOPHP 2019), Daejeon, Korea: 2019.
[58] M. Slobodeniuk, R. Bertossi, V. Ayel, R. Ravichandran, K. Thyagarajan, C. Romestant, et al., Experimental study of the flat plate pulsating heat pipe operation during dry-out and flow re-activation periods under microgravity conditions, Int. J. Multiph. Flow 147 (2022) 103888, https://doi.org/10.1016/j.ijmultiphaseflow.2021.103888.
[59] A. Cecere, G.D. Di Martino, S. Mungiguerra, Experimental Investigation of Capillary-Driven Two-Phase Flow in Water/Butanol under Reduced Gravity Conditions, Microgravity Sci. Technol. 31 (2019) 425–434, https://doi.org/10.1007/s12217-019-09723-9.
[60] V. Ayel, L. Pietrasanta, G. Lalizel, C. Romestant, Y. Bertin, M. Marengo, Thermo-Hydraulic Analysis of Semi-Transparent Flat Plate Pulsating Heat Pipes Tested in 1 g and Microgravity Conditions, Microgravity Sci. Technol. 31 (2019) 403–415, https://doi.org/10.1007/s12217-019-9701-6.
[61] V. Ayel, L. Araneo, P. Marzorati, C. Romestant, Y. Bertin, M. Marengo, Visualization of Flow Patterns in Closed Loop Flat Plate Pulsating Heat Pipe Acting as Hybrid Thermosyphons under Various Gravity Levels, Heat Transfer Eng. 40 (2019) 227–237, https://doi.org/10.1080/01457632.2018.1426244.
[62] M. Abela, M. Mameli, V. Nikolayev, S. Filippeschi, Experimental analysis and transient numerical simulation of a large diameter pulsating heat pipe in microgravity conditions, Int. J. Heat Mass Transf. 187 (2022) 122532, https://doi.org/10.1016/j.ijheatmasstransfer.2022.122532.
[63] M. Mameli, S. Piacquadio, A.S. Viglione, A. Catarsi, C. Bartoli, M. Marengo, et al., Start-Up and Operation of a 3D Hybrid Pulsating Heat Pipe on Board a Sounding Rocket, Microgravity Sci. Technol. 31 (2019) 249–259, https://doi.org/10.1007/s12217-019-9682-5.
[64] T.T.T. Nguyen, J. Yu, P.C. Wayner, J.L. Plawsky, A. Kundan, D.F. Chao, et al., Rip currents: A spontaneous heat transfer enhancement mechanism in a wickless heat pipe, Int. J. Heat Mass Transf. 149 (2020) 119170, https://doi.org/10.1016/j.ijheatmasstransfer.2019.119170.
[65] J. Yu, T.T.T. Nguyen, A. Pawar, P.C. Wayner, J.L. Plawsky, D.F. Chao, et al., The effect of condenser temperature on the performance of the evaporator in a wickless heat pipe performance, Int. J. Heat Mass Transf. 176 (2021) 121484, https://doi.org/10.1016/j.ijheatmasstransfer.2021.121484.
[66] H. Zhang, G. Li, L. Chen, G. Man, J. Miao, X. Ren, et al., Development of Flat-Plate Loop Heat Pipes for Spacecraft Thermal Control, Microgravity Sci. Technol. 31 (2019) 435–443, https://doi.org/10.1007/s12217-019-09716-8.
[67] C. Tarau, M.T. Ababneh, W.G. Anderson, A.R. Alvarez-Hernandez, S. Ortega, J. T. Farmer, et al., Advanced Passive Thermal eXperiment (APTx) for Warm-Reservoir Hybrid-Wick Variable Conductance Heat. Pipes on the International Space Station (ISS). 48th International Conference on Environmental Systems, 2018.
[68] R. Clavenna, L. Araneo, V. Dupont, R. Boubaker, Capillary Jet Loop performance in parabolic flight, Appl. Therm. Eng. 217 (2022) 119221, https://doi.org/10.1016/j.applthermaleng.2022.119221.
[69] M. Mameli, A. Catarsi, D. Mangini, L. Pietrasanta, N. Michè, M. Marengo, et al., Start-up in microgravity and local thermodynamic states of a hybrid loop thermosyphon/pulsating heat pipe, Appl. Therm. Eng. 158 (2019) 113771, https://doi.org/10.1016/j.applthermaleng.2019.113771.
[70] L. Pagliarini, L. Cattani, F. Bozzoli, M. Mameli, S. Filippeschi, S. Rainieri, et al., Thermal characterization of a multi-turn pulsating heat pipe in microgravity

conditions: Statistical approach to the local wall-to-fluid heat flux, Int. J. Heat Mass Transf. 169 (2021) 120930, https://doi.org/10.1016/j.ijheatmasstransfer.2021.120930.
[71] P.E. Beck, L.P.M. Brendel, J.E. Braun, E.A. Groll, P.E. Beck, L.P.M. Brendel, et al., Investigation of Two-phase Refrigerant Behavior Upon Cycle Startup for Compressor Protection in Microgravity Applications. International Refrigeration and Air Conditioning Conference, 2021.
[72] J.M. Ezquerro, A. Bello, P. Salgado Sánchez, A. Laveron-Simavilla, V. Lapuerta, The Thermocapillary Effects in Phase Change Materials in Microgravity experiment: Design, preparation and execution of a parabolic flight experiment, Acta Astronaut. 162 (2019) 185–196, https://doi.org/10.1016/j.actaastro.2019.06.004.
[73] J.M. Ezquerro, P. Salgado Sánchez, A. Bello, J. Rodríguez, V. Lapuerta, A. Laveron-Simavilla, Experimental evidence of thermocapillarity in phase change materials in microgravity: Measuring the effect of Marangoni convection in solid/liquid phase transitions, Int. Commun. Heat Mass Transfer 113 (2020) 104529, https://doi.org/10.1016/j.icheatmasstransfer.2020.104529.
[74] H.-S. Roh, Heat transfer mechanisms in pool boiling, Int. J. Heat Mass Transf. 68 (2014) 332–342, https://doi.org/10.1016/j.ijheatmasstransfer.2013.09.037.
[75] S.K. Singh, D. Sharma, Review of pool and flow boiling heat transfer enhancement through surface modification, Int. J. Heat Mass Transf. 181 (2021) 122020, https://doi.org/10.1016/j.ijheatmasstransfer.2021.122020.
[76] D.G. Gilmore, Spacecraft thermal control handbook, Aerospace Press (2002).
[77] Brendel L, Groll E, M Brendel LP, Caskey SL, Ewert MK, Gomes AR, et al. Equivalent Mass Benefits from Employing Vapor Compression Refrigeration on Spacecraft. 2021.
[78] Engineers EDGE. Steady Flow Vapor-Compression Refrigeration Cycle - Class 14 n.d.
[79] P. Salgado Sánchez, J.M. Ezquerro, J. Porter, J. Fernández, I. Tinao, Effect of thermocapillary convection on the melting of phase change materials in microgravity: Experiments and simulations, Int. J. Heat Mass Transf. 154 (2020) 119717, https://doi.org/10.1016/j.ijheatmasstransfer.2020.119717.
[80] G. Nobrega, R.R. de Souza, I.M. Gonçalves, A.S. Moita, J.E. Ribeiro, R.A. Lima, Recent Developments on the Thermal Properties, Stability and Applications of Nanofluids in Machining, Solar Energy and Biomedicine. Applied Sciences (switzerland) 12 (2022), https://doi.org/10.3390/app12031115.
[81] X. Fang, Y. Chen, H. Zhang, W. Chen, A. Dong, R. Wang, Heat transfer and critical heat flux of nanofluid boiling: A comprehensive review, Renew. Sustain. Energy Rev. 62 (2016) 924–940, https://doi.org/10.1016/j.rser.2016.05.047.
[82] R.R. Souza, F.M. Sá Barbosa, G. Nobrega, E.M. Cardoso, J.C.F. Teixeira, A. S. Moita, et al., Experimental study of an innovative elastomer-based heat exchanger, Case Stud. Therm. Eng. 49 (2023) 103365, https://doi.org/10.1016/j.csite.2023.103365.
[83] S. Li, J. Zhang, J. He, W. Liu, Y. Wang, Z. Huang, et al., Functional PDMS Elastomers: Bulk Composites, Surface Engineering, and Precision Fabrication, Adv. Sci. 10 (2023), https://doi.org/10.1002/advs.202304506.
[84] E. Freitas, P. Pontes, R. Cautela, V. Bahadur, J. Miranda, A.P.C. Ribeiro, et al., Pool Boiling of Nanofluids on Biphilic Surfaces: An Experimental and Numerical Study, Nanomaterials 11 (2021) 125, https://doi.org/10.3390/nano11010125.
[85] H. Tarigonda, D.P.M.D. Shaik, D.R.R. Reddy, G.V.S. Reddy, Experimental Investigation on the Heat Pipe using Al2O3 and CuO Hybrid Nanofluid, Int. J. Thermophys. 43 (2022) 153, https://doi.org/10.1007/s10765-022-03078-x.
[86] M.M. Sarafraz, A.T.K. Abad, Statistical and experimental investigation on flow boiling heat transfer to carbon nanotube-therminol nanofluid, Physica A 536 (2019) 122505, https://doi.org/10.1016/j.physa.2019.122505.
[87] B. Eanest Jebasingh, A.A. Valan, A comprehensive review on latent heat and thermal conductivity of nanoparticle dispersed phase change material for low-temperature applications, Energy Storage Mater. 24 (2020) 52–74, https://doi.org/10.1016/j.ensm.2019.07.031.
[88] Y. Ji, G. Liu, H. Ma, G. Li, Y. Sun, An experimental investigation of heat transfer performance in a polydimethylsiloxane (PDMS) oscillating heat pipe, Appl. Therm. Eng. 61 (2013) 690–697, https://doi.org/10.1016/j.applthermaleng.2013.09.001.
[89] M. Mohan, S. Thomas, C.B. Sobhan, Convective heat transfer estimation of dilute metal oxide nanofluids in VUV surface tuned minichannel using Mach-Zehnder interferometry, Appl. Therm. Eng. 196 (2021) 117259, https://doi.org/10.1016/j.applthermaleng.2021.117259.
[90] A.V. Macatangay, K.S. Prokhorov, J.J. Sweterlitsch, Strategies to Mitigate Ammonia Release on the International Space Station, SAE Trans. 116 (2007) 344–355.
[91] P.R. Tete, M.M. Gupta, S.S. Joshi, Developments in battery thermal management systems for electric vehicles: A technical review, J Energy Storage 35 (2021) 102255, https://doi.org/10.1016/j.est.2021.102255.
[92] Birur GC, Johnson KR, Novak KS, Sur TW. Thermal Control of Mars Lander and Rover Batteries and Electronics Using Loop Heat Pipe and Phase Change Material Thermal Storage Technologies, 2000. https://doi.org/10.4271/2000-01-2403.
[93] A.D. Pathak, S. Saha, V.K. Bharti, M.M. Gaikwad, C.S. Sharma, A review on battery technology for space application, J Energy Storage 61 (2023) 106792, https://doi.org/10.1016/j.est.2023.106792.
[94] Pandey G. Chandrayaan-3: Indian space agency Isro says no signal yet from Moon lander. BBC 2023. https://www.bbc.com/news/world-asia-india-66893924 (accessed November 21, 2023).
[95] J.A. Supowit, C.H. Baker, Thermal Diode Design Concept for High Power Density Spacecraft. 47th International Conference on Environmental Systems, 2017.
[96] M.Y. Wong, Y. Zhu, Y. Zeng, T.C. Ho, Y. Yang, H. Qiu, et al., Thermal Rectification Enhancement of Coalescence-Jumping Phase Transition Thermal Diodes using Cu–Al2O3 Hybrid Nanofluids, Adv. Eng. Mater. 24 (2022), https://doi.org/10.1002/adem.202100958.
[97] D. Tian, Y. Song, L. Jiang, Patterning of controllable surface wettability for printing techniques, Chem. Soc. Rev. 42 (2013) 5184, https://doi.org/10.1039/c3cs35501b.
[98] S.M. Oliveira, W. Song, N.M. Alves, J.F. Mano, Chemical modification of bioinspired superhydrophobic polystyrene surfaces to control cell attachment/proliferation, Soft Matter 7 (2011) 8932, https://doi.org/10.1039/c1sm05943b.
[99] R. Ul Hassan, J. Lee, S.M. Khalil, G. Kang, D.-H. Cho, D. Byun, Experimental, Theoretical, and Numerical Investigation of the Electric Field and Surface Wettability Effects on the Penetration Length in Capillary Flow, ACS Omega 6 (2021) 32773–32782, https://doi.org/10.1021/acsomega.1c04629.
[100] X.-Q. Chen, L. Tong, Multiscale flow characteristics of droplet spreading with microgravity conditions, Can. J. Phys. 97 (2019) 869–874, https://doi.org/10.1139/cjp-2018-0474.
[101] B. Liu, I. Khalid, I. Patra, O.R. Kuzichkin, R. Sivaraman, A. Turki Jalil, et al., The effect of hydrophilic and hydrophobic surfaces on the thermal and atomic behavior of ammonia/copper nanofluid using molecular dynamics simulation, J. Mol. Liq. 364 (2022) 119925, https://doi.org/10.1016/j.molliq.2022.119925.
[102] X. Liu, M. Adibi, M. Shahgholi, I. Tlili, S. Mohammad Sajadi, A. Abdollahi, et al., Phase change process in a porous Carbon-Paraffin matrix with different volume fractions of copper oxide Nanoparticles: A molecular dynamics study, J. Mol. Liq. 366 (2022) 120296, https://doi.org/10.1016/j.molliq.2022.120296.
[103] P. Jarmatz, H. Wittenberg, V. Jafari, A. Das Sharma, F. Maurer, N. Wittmer, et al., MaMiCo 2.0: An enhanced open-source framework for high-performance molecular-continuum flow simulation, SoftwareX 20 (2022) 101251, https://doi.org/10.1016/j.softx.2022.101251.